12-3-2020

Inter-Annual to Inter-Decadal Spatiotemporal Effects of Storm and Nourishment Events in North Myrtle Beach, South Carolina

Christina Mary Boyce
Coastal Carolina University

Inter-Annual to Inter-Decadal Spatiotemporal Effects of Storm and Nourishment Events in North Myrtle Beach, South Carolina

---

By: Christina Mary Boyce

Submitted in Partial Fulfillment of the Requirements for the Degree of Master of Science in Coastal Marine and Wetland Studies in the Department of Marine Science School of the Coastal Environment

Coastal Carolina University

Fall 2020

X

Dr. Paul Gayes, Major Professor

X

Dr. Erin Hackett, Committee Member

X

Dr. Patrick Limber, Committee Member

X

Dr. C. Robin Mattheus, Committee Member

X

Dr. William Houston, Committee Member

X

Dr. Richard Viso, Committee Member

X

Dr. Richard Viso, Department Coordinator

X

Dr. Michael Roberts, Dean

Dedication

I would like to dedicate this thesis to my grandma Mary Olivarez. You lived a life full of giving, hope, and selflessness and I am so proud to be your granddaughter. I will miss your baked mostaccioli and your funny sayings, but most of all, I will miss you. I wish you were here with me to celebrate this milestone in my life as I know you would be so proud of me, but I know you are with me in spirit. I love you.

Wise advise from my grandma Mary:

'Be true to your teeth or they will be false to you.'

And

'Don't take any wooden nickels.''

Acknowledgements

First, I would like to thank my advisor, Dr. Paul Gayes, for taking me on as a student. The opportunities that you have presented me have formed into a professional who is able to view a complex problem from many different angles. Second, I would like to greatly thank everyone on my committee which includes Dr. Hackett, Dr. Limber, Dr. Viso, Dr. Mattheus, and Dr. Houston. Each one of you has helped me one way or another on this journey and your efforts do not go unappreciated. Third, I would like to thank the CMWS and CMSS graduate students, especially those in the Burroughs and Chapin Center for Marine and Wetland Studies and Environmental Fluids Lab, for all your love and support. And last, a big shoutout to the City of North Myrtle Beach and the South Carolina Ocean Coastal Resource Management division for allowing us to continue the Beach Erosion Research Monitoring (BERM) program.

Abstract

Inter-annual to inter-decadal spatial and temporal changes in morphology a the nearshore system in relation to large storm and nourishment events of the Grand Strand, SC, is assessed using a 23-year time series of beach elevation profiles collected at North Myrtle Beach, SC in addition to multibeam bathymetry and backscatter intensity. Beach profiles are used for volume and empirical orthogonal function (EOF) analysis to extract spatiotemporal trends in the cross-shore and longshore directions to determine a sediment budget and to identify dominate morphological changes. Volume analysis found an overall increase in total volume for the study period compared to the initial 1996 pre-nourishment survey with ~82% of total nourishment volume placed since 1996 remaining in the system. Strong evidence of cross-shore transport is found within subsection volume analysis and within mode one of the EOF analysis. Mode one also highlights the distribution of nourishment sediment after its been placed and the effects storms. Mode two of the EOF analysis highlights longshore changes across the study site due to fluctuation of Hog Inlet. These changes, which typically are only observed in proximal beach elevation profile to the inlet, can be observed at greater longshore distances away from the inlet, differing from the South Carolina Ocean and Coastal Resource Management's definition of an 'inlet hazard zone'. In addition, mode two identifies the effect of storms on the inlet. Cuspate features identified in multibeam analysis at the shoreface-to-shelf transition zone may be a sediment source for the offshore due to textural differences between geologic units.

Table of Contents

List of Tables

List of Figures

List of Symbols

$\boldsymbol{A}$ – data matrix for EOF analysis

$b_i(t)$ – temporal coefficient

C_{su}– cross correlation coefficient

d_1 – distant to updrift profile (

d_2 – distant to downdrift profile

e – set of transects through time

$\bar{e}$ – mean of transect through time

l – discrete lag

N – total samples

n_t – number of surveys

$\boldsymbol{R} = \boldsymbol{\vartheta\beta}$

$R_i(t)$ – temporal coefficients or principal components (PC)

r_s – profile area

S – sample from bathymetry survey 1

$\bar{S}$ – mean of sample from bathymetry survey 1

T – matrix transpose

t – survey number

U – sample from bathymetry survey 2

$\overline{U}$ – mean of sample from bathymetry survey 2

v_s – profile volume

x– vectorized data points in cross-shore direction for survey number, *t*

z – elevation contour

$\boldsymbol{\beta}$ - an $t \times x$ matrix with zero components except along the diagonal which are the singular values of $\boldsymbol{A}$

δ - Pearson's correlation coefficient

$\boldsymbol{\varepsilon}$ - an $x \times x$ orthogonal matrix that represents the mode functions

$\varepsilon_i(x)$ – spatial coefficients or modes

θ – half-cell subsection volume

$\bar{\theta}$ – mean of half-cell subsection volume through time

$\rho_i(x)$ – spatial eigenfunctions (or modes)

σ – standard deviation of transects

τ – p-value with 2 degrees of freedom for *z*

$\boldsymbol{\vartheta}$ – an $t \times t$ orthogonal matrix

ω – half-cell subsection volume

$\bar{\omega}$ - mean of half-cell subsection volume through time

List of Acronyms

BCCMWS – Burroughs and Chapin Center for Marine and Wetland Studies

BERM – Beach Erosion Research and Monitoring

CCU – Coastal Carolina University

DHEC – Department of Health and Environmental Control

DoC – Depth of closure

EOF – Empirical Orthogonal Function

NAVD 88 - North American Vertical Datum of 1988

NOAA – National Oceanic and Atmospheric Administration

NMB – North Myrtle Beach

OCRM – Ocean and Coastal Resource Management

PC – Principal component

PCA – Principal component analysis

PSD – Power spectral density

RTK-GPS – Realtime kinematic global positioning system

SC – South Carolina

SVD – Singular value decomposition

T - Transect

1. Introduction

Understanding coastal systems requires comprehensive knowledge of processes that occur over different scales of space and time (Southgate et al., 2003). The need for understanding is even greater as populations are increasing in coastal communities, where local governments are under greater pressure to deal with protecting life and property from sea-level-rise and storm events (Kulp and Strauss, 2019; Neumman et al., 2015). One growing area that would benefit from a long-term coastal change analysis is the Grand Strand of South Carolina (Figure 2), which was the second fastest growing region in the United States from 2012-2017 (South Carolina Flood Commission, 2019). The Grand Strand has an economy linked to the overall stability of its beaches (Denny et al., 2005), which rely on beach nourishments as the main source of erosion control since the construction of new hard structures is prohibited (McCoy et al., 2010). As of 2019, four major nourishment projects have been conducted in the Grand Strand (Table 1). In addition to nourishments, the southeast coast of the United States was frequently struck by tropical storms and hurricane events with higher frequency years occurring from 2002 to 2006 and 2015 to 2019 (Table 2; Figure 1). Thus, interdecadal morphology of the beach system and its response to successive hurricane events and repeated nourishment must be assessed.

Documenting changes of coastal morphology over interannual to decadal scales is needed to aid beach managers in planning and making beach-protection strategies. These changes have additional implications for coastal ecosystems, which are experiencing temperature and other physical and biogeochemical responses to climate change on these times scales. To assess morphological change, a 23-year time series of beach elevation profiles from North Myrtle Beach, SC, is used for volume and empirical orthogonal

function (EOF) analysis as tools for assessing change over the study period in addition to storm and nourishment impact (Bochev-van der Burgh et al, 2009; Díez et al., 2018; Farris and List, 2007). Wind data collected from a local airport and three multibeam bathymetry and backscatter surveys from the shoreface-to-shelf transition zone, collected after and between large storm events are used for context in analysis.

2. Study Area

2.1 Physical Setting

North Myrtle Beach (NMB) lies within the Grand Strand of South Carolina (Figure 2), a 100 km stretch of coast from the North Carolina/South Carolina border at Little River Inlet to the mouth of Winyah Bay. The Grand Strand is within Long Bay, a large crescentic shaped embayment extending from Cape Fear, North Carolina to Cape Romain, South Carolina with an overall shoreline orientation in the SW-NE direction. Dominate wind patterns within the Grand Strand vary due to seasonal changes but follow the same, predominately alongshore, SE-NE orientation (Barnhardt, 2009; Denny et al., 2013; Dolan, 2016; Slovinsky, 2001), with the northern component slightly more dominate (Kana et al., 2013). Locally, at the NMB study site, Kana et al. (2013) did find bi-modal wind patterns within the study site with a northern wind component near Hog Inlet, and a southern component further south within the study area. The tidal range is microtidal with a mean tidal range of 1.5 m (Barnhardt, 2009; Slovinsky, 2001). This region is sediment starved, receiving little input from nearby rivers (Gayes et al., 2003). Despite of the lack of sediment, annual shoreline erosion rates are, on average, relativity low (<<1m/y) (Park, Gayes, and Wells, 2009). The Grand Strand is typically characterized by a headland coast in the central area centered on the city of Myrtle Beach, South Carolina, with barrier

island chains extending south of Murrells Inlet and northeast of NMB (Dolan, 2016; Figure 2). NMB is a ~13 km coastline located in the northern section of the Grand Strand that is flanked by Hog Inlet, an intermediate tidal inlet with a net longshore sediment to the northeast (Kana et al., 2013). White Point Swash, a small tidal swash in a vestigial estuarine system, forms the southwest boundary of the study area and experiences a net southwesterly longshore transport (Kana et al, 2013). The City of North Myrtle Beach area has received many nourishments, however, the first major nourishment took place in 1996 with subsequent events taking place in in 2008, 2017, and 2018 (Table 1).

2.2 Geologic Setting

The Grand Strand lies just southwest of the main axis of the Cape Fear Arch (or Mid-Carolina Platform High), a large dome composed of basement rock that began uplifting during the late-Cretaceous/early-Tertiary (Baldwin et al., 2004; Denny et al., 2015; Dolan, 2016; Park, Gayes, and Wells, 2009). The shape of the Cape Fear Arch has played a major role in sedimentation patterns by diverting Pleistocene and Holocene age sediment away from the Grand Strand region (Baldwin et al., 2004; Park, Gayes, and Wells, 2009). Sea-level fluctuations during the Cretaceous and Tertiary caused deep paleo-channels to incise through the southern dipping strata that were later filled in by coarse Pleistocene age sediment (Baldwin et al., 2004; Barnhardt, 2009). Pleistocene sea-level fluctuations later caused a regional unconformity, truncating the infilled paleo-channels, exposing Cretaceous and Tertiary deposits, and depositing river-derived sediments as beach-barrier complexes upland (Baldwin et al., 2004; Barnhardt, 2009; Denny et al., 2015). Modern fine-grained Holocene sediments are limited and exist as a thin discontinuous

veneer ranging from less than 0.5 m to 6 m in thickness throughout the shoreface and inner-shelf (Barnhardt, 2009; Denny et al., 2015).

3. Methodology

3.1 Data

Beach-elevation profiles are a common coastal dataset employed to examine morphological changes and interactions between the nearshore and offshore environments (Farris and List, 2007; Park, Gayes, and Wells, 2009). Although beach profiles lack the spatial resolution in the alongshore direction to resolve small-scale variance in alongshore beach morphology (Theuerkauf and Rodriguez, 2012), they typically comprise larger temporal datasets covering the entire active beach. This feature makes them useful in determining inter-annual to inter-decadal changes within an active beach.

A 23-year subset (1996-2019) of beach profile data from North Myrtle Beach, SC (Table 2) is used for spatial and temporal volume and EOF analysis at 39 South Carolina Ocean and Coastal Resource Management (OCRM) transect locations (Figure 2). These profiles are perpendicular to the shoreline and, on average, are 300 m apart in the longshore direction. Transects are typically 1 km in length and originate behind the dune field and extend past the lower shoreface into the inner-shelf. Data was collected by the Beach Erosion Research and Monitoring (BERM) program conducted by the Burroughs and Chapin Center for Marine and Wetland Studies at Coastal Carolina University (BCCMWS-CCU) and the SC OCRM. Profiles are referenced to the North American Vertical Datum of 1988 (NAVD 88). Profiles were collected using a combination of on-land real-time kinematic global positioning systems (RTK-GPS) and offshore Knudsen single beam echosounder measurements with horizontal and vertical maximum errors of ±3 and ± 6 cm,

respectively (Park, Gayes, and Wells, 2009). A total of 25 surveys from 1996 to 2019 are used in this study. Surveys were collected at various times of the year, including before and after beach nourishments and major storms. Due to spatial limitations, multibeam bathymetry and backscatter intensity data, collected by the CCU-BCCMWS are used to provide context for interpretations of volume and other statistical analyses to aid in the assessment of spatial change.

To determine if temporal and spatial change is related to wind direction and intensity, data measuring daily wind speed and wind direction were collected at the Grand Strand Airport in North Myrtle Beach, SC, and sourced from the U.S. Local Climatological Data through the National Oceanic and Atmospheric Administration (NOAA) National Centers for Environmental Information (https://www.ncei.noaa.gov/access/search/data-search/local-climatological-data) (Figure 2). Data from June 15, 1999, until December 31, 2019, is used in this study to examine long term averages of wind speed and direction. Coverage of wind data does not predate June 15,1999. Due to the proximity of the Grand Strand Airport to the study site, winds at the airport are assumed to be the same as within the study site (Figure 2). Wind data are broken up by year to determine if they are at a steady longshore direction and/or if wind direction changes interannually. This wind analysis represents a proxy for the local wave field, particularly the waves associated with a seasonally intense sea breeze system and does not include swell components of the wave field as there are no long-term wave gauge stations covering the study period near the study site. Monthly averages of wind speed and direction are also computed and presented to evaluate seasonal changes throughout the study period.

Storm events, documented in *Table 2*, are determined from named tropical cyclone and hurricane history provided by the SC NOAA National Weather Service Charleston office (https://www.weather.gov/chs/TChistory) (Figure 3). In addition to tropical storm and hurricanes that impacted South Carolina, Hurricane Florence (Sep 2018) was added to the dataset as it made landfall near Wilmington, NC, ~100 km north of the study site. Hurricane and tropical storm tracks were sourced from NOAA National Centers for Environmental Information (https://www.ncdc.noaa.gov/ibtracs/index.php?name=ib-v4-access).

3.2 Beach-Profile Analysis and Sediment Volume Calculations

Prior to statistical analysis, individual beach profiles are evaluated to examine temporal change. Due to the quantity and similarity of adjacent profiles, three transects, Transect 2, Transect 20, and Transect 39, are selected to represent the southern, mid, and northern sections of the study site, respectively. For the three selected profiles, standard deviation with respect to time-averaged beach profile of the elevation profiles over time are computed to determine variance (Larson and Kraus, 1994):

$$\sigma = \sqrt{\frac{\sum_{i=1}^{n_t}(e_i - \bar{e})^2}{n_t - 1}} \qquad (1)$$

where n_t is the number of surveys, e is elevation at a single location in the cross-shore direction from a transect, $\bar{e}$, is the average of the time series of one location in the cross-shore direction from a transect.

Volumes of each profile (v_s) are calculated using the half-cell method:

$$v_s = r_s(\frac{d_1}{2} + \frac{d_2}{2}) \quad (2)$$

where r_s is the cross-sectional area of each cross-shore profile, d_1 is the distance to the updrift adjacent profile, and d_2 is the distance to the downdrift adjacent profile (Figure 4). Volumes of profiles found on the northern and southern edges of the study area (Transect 1 and Transect 39) are determined using a modified form of Equation 2:

$$(v_s) = (r_s)\left(\frac{d_1}{2}\right) \quad (3)$$

where only one distance term is used to avoid extrapolation to areas outside the study area.

The sum of the half-cell volumes for each profile comprises the total profile volume. Half-cell volumes are also broken into subsections representing morphological boundaries by profile elevation (z) contour intervals including: the backshore (z > 0.5 m), foreshore (0.5 m < z ≤ -1.2 m), upper shoreface (-1.2 m < z ≤ -3 m), lower shoreface (-3 m < z ≤ -5 m), upper offshore (-5 m < z ≤ -6 m), and offshore (z < -6 m) (Park, Gayes, and Wells, 2009; Figure 5). To determine change through time for total volumes and subsection volumes, volume differences are referenced to the initial Jan-96 elevation survey. The Pearson correlation coefficient is calculated between half-cell volumes of two subsections over time to determine if a relationship between subsections exists. The correlation coefficient, δ, is:

$$\delta_{\theta\omega} = \frac{\sum_{i=1}^{N}(\theta_i - \bar{\theta})(\omega_i - \bar{\omega})}{\sqrt{\sum_{i=1}^{N}(\theta_i - \bar{\theta})^2}\sqrt{\sum_{i=1}^{N}(\omega_i - \bar{\omega})^2}} \quad (4)$$

where θ represents the half-cell volume of one subsection, ω represents the half-cell volume of another subsection, $\bar{\theta}$ and $\bar{\omega}$ are the means of each subsection, respectively, and *N* is the number of half-cell volumes or the number of elevation surveys. Correlation coefficients are computer for half-cell volumes estimated from the entire elevation profile as well as those estimated for each subsection.

Significance values, τ , for each associated correlation coefficient are calculated to determine the significance of each subsection volume relationship using the t-distribution with *N*-2 degrees of freedom:

$$\tau = \frac{\delta\sqrt{N-2}}{\sqrt{1-\delta^2}} \tag{5}$$

p-values smaller than 0.05 are considered significant.

3.3 Empirical Orthogonal Functions of Beach Elevation Profiles

EOF analysis, also known as principal component analysis (PCA), is a mathematical technique used to extract underlying patterns within a dataset (Bochev-van der Burgh et al, 2009; Díez et al., 2018; Farris and List, 2007). The use of modern technology has broadened the application of this method in many fields of study and has been used extensively in the geoscience field to evaluate major trends in spatio-temporal variability in geophysical data, such as beach elevation profiles, to help characterize changes in beach elevations in both cross-shore and longshore directions through time (Díez et al., 2018; Lemke, Miller, and Gorton, 2014; Ludka et al., 2015; Miller and Dean, 2007; Young and Park, 2018). Dominant elevation changes identified via EOF analyses may be attributed to physical processes (Díez et al., 2018;

Hapke et al, 2010; Ludka et al., 2015; Young and Park, 2018). In this study, EOF analysis is used to extract underlying patterns within the 25 elevation surveys (1996-2019), conducted for each of the 39 NMB transects.

EOF analysis decomposes the data into eigenfunctions, or modes, which optimally decompose the variance within space or time. Each mode is composed of an eigenvector, a principal component (PC), and an eigenvalue (Figure 6). For this study, spatial patterns of variability are described by the eigenvectors while the PC describe temporal variability of each eigenvector. Eigenvalues rank the variance, or weight, associated with each mode, where mode one represents the most variance within the profile elevation data while subsequent higher modes represent lesser and lesser variability.

Prior to the EOF analysis, all transect origin points are adjusted to begin at the 2016-2019 SC OCRM Beachfront Jurisdictional baseline. By adjusting the transects, the natural curvature of the shoreline is accounted for as well as slight offsets in the layout of the original OCRM transect locations relative to a coast parallel or morphologically based baseline. As a result, this procedure facilitates comparison of similar morphologies to a consistent baseline. Measured transects are interpolated to 1-meter resolution using the nearest neighbor method to ensure equal spacing, and profiles are clipped to cover the same range (627 m from the baseline) in the offshore direction. Missing data points due to lack of spatial coverage or failure of equipment were linearly interpolated over time. Mean temporal profiles of each transect are then removed to better ascertain variability as the mean typically describes the majority of the variance in beach profiles (Bochev-van der Burgh et al., 2009). By removing the temporal mean profile from each transect, each mode will describe deviations from the mean profiles (Bochev-van der Burgh et al., 2009).

In order to analyze both longshore and cross-shore processes throughout the study period, the 39 transect from one survey period are concatenated. By removing the temporal mean profile from each transect prior to concatenation, the introduction of variance is minimized. The data are subsequently arranged into a matrix $\boldsymbol{A}(\boldsymbol{x},\boldsymbol{t})$, where elevations along each row represent those from each cross-shore position (x) of the concatenated transects (of which there 627 positions per transect × 39 transects = a total of 24,453 positions) and elevations along the columns represent the survey dates, or time (t) (of which there are a total of 25. The singular value decomposition (SVD) of matrix **A** is computed:

$$\boldsymbol{A} = \vartheta\beta\varepsilon^{T} \tag{6}$$

where $\boldsymbol{\vartheta}$ is an $t \times t$ orthogonal matrix, $\boldsymbol{\beta}$ is an $t \times x$ matrix with zero components except along the diagonal, which are the singular values of **A**, $\boldsymbol{\varepsilon}$ is an $x \times x$ orthogonal matrix that represents the mode functions, and T indicates matrix transpose. If $\boldsymbol{R} = \boldsymbol{\vartheta\beta}$, then,

$$\boldsymbol{A} = R\varepsilon^{T} = \sum_{i=1}^{x} R_i(t)\varepsilon_i(x) \tag{7}$$

where $R_i(t)$ are the temporal coefficients, or principal components (PC), $\varepsilon_i(x)$ are the spatial coefficients, or modes. The i^{th} singular value divided by the sum of all singular values represents the relative contribution of the i^{th} mode. Modes and PC's are normalized by their standard deviation. It is important to note that modes are orthonormal from one another in space and time, and mode functions may not always represent a physical process (Dommenget and Latif, 2002).

3.4 Multibeam Analysis

Multibeam surveys were performed in March 2017, March 2018, and January 2019 to characterize ~13 km of the lower shoreface/inner-shelf of NMB. In addition to volume change, multibeam bathymetry and backscatter intensity will aid in determining high resolution spatial analysis in overlapping subsections to better understand spatial characteristics. Multibeam data were collected using a 300 kHz duel-head Kongsberg system. Sound velocity profiles were collected at the beginning of each multibeam survey and GPS heading and vessel heave, pitch, and roll are collected simultaneously. Post processing is performed in CARIS 10.2 which allows for the application of a tidal correction and swath-by-swath data point editing at a 0.5-m resolution. Geotiffs of backscatter intensity and bathymetry of each multibeam survey are transferred to ArcMap 10.5.1 for volumetric and change analysis of the lower shoreface/inner-shelf.

In addition to bathymetry differences, cross correlation function analysis between the multibeam bathymetric surveys along three longshore transects is performed. This analysis determines if horizontal shifts in volume over time are present at a high spatial resolution by analyzing periodicities within the bathymetry data. To prepare bathymetric data for cross-correlation, the contours of the January 2019 multibeam bathymetry geotiff are determined at 1-meter resolution. Three transect lines are created between the -4 m and -5 m, -5 m and -6 m, and -6 m and -7 m contour intervals of the January 2019 survey, representing the lower shoreface, upper offshore, and offshore subsections, respectively. These transects are ~9 km in length and represent ~65% of the offshore distance covered in the study area. Full coverage could not be completed as the three multibeam surveys did not fully overlap with one another. For each survey, multibeam

bathymetry points along each transect line are extracted at 0.5 m spacing. Data gaps in the multibeam swaths are linearly interpolated.

Bathymetry extractions are linearly detrended and broken into 2000 m segments from SW to NW with 50% overlap, truncating data into even segments. For each contour interval, correlation function analysis is performed between two different bathymetric surveys for each 2000 m segment. Cross correlations functions (C_{su}) between two bathymetric survey periods for one segment are calculated:

$$C_{su}(l) = \frac{\sum_{i=1}^{N-|l|}(S_{i+l} - \bar{S})(U_i - \bar{U})}{[\sum_{i=1}^{N}(S_i - \bar{S})^2]^{\frac{1}{2}}[\sum_{i=1}^{N}(U_i - \bar{U})^2]^{\frac{1}{2}}} \quad l \geq 0$$

$$C_{su}(l) = \frac{\sum_{i=1+|l|}^{N}(S_{i+l} - \bar{S})(U_i - \bar{U})}{[\sum_{i=1}^{N}(S_i - \bar{S})^2]^{\frac{1}{2}}[\sum_{i=1}^{N}(U_i - \bar{U})^2]^{\frac{1}{2}}} \quad l < 0 \tag{8}$$

Where l is discrete lag in the cross-shore direction, N is the number of points in each segment, S is elevation segments of survey 1,$\bar{S}$ is the segment spatial mean elevation of survey 1, U is elevation segments of survey 2 and $\bar{U}$ is the segment mean elevation of survey 2. The correlation coefficients are subsequently averaged over all segments for each analysis to reduce noise calculating a total of 9 correlation functions (3 survey dates for 3 transects after averaging).

4. Results

4.1 Wind Data

Yearly and multi-year wind rose diagrams from the Grand Strand NMB airport from June 15, 1999 to December 31st, 2019 show there are three main wind directions throughout the time period observed (Figure 7). The dominate wind direction originates from the southwest between 210° and 230°. The secondary direction originates from the northeast between 30° and 60° while the third direction originates from the east-southeast between 90° and 120°. The dominate daily wind speed for the three main wind directions are between 2 m/s and 5 m/s. For each observed year, the trimodal pattern largely remains consistent except for years 2008, 2014, and 2016 where east-southeast originated winds are not as common.

To better estimate the potential influence of storm events, monthly averages of wind speed and direction are calculated given that periods of intense storms should increase the average wind speed (Figure 8). A cyclic pattern is observed in the monthly data with larger wind speeds being observed near storm events which can be found in *Table 2*.

4.2 Beach Profile Variability

For many applications, the seaward boundary of the active littoral zone is defined by the critical depth or depth of closure (DoC) and used to delineate the seaward extent of an "active beach system" from the inner shelf which is presumed to be a sink for beach volume (Kraus and Harikai, 1999). DoC can be defined by the average significant wave height over a defined period, typically a year, (Hallermeier, 1981; Kana et al., 2013) or morphologically. Here, we determine the DoC at the NMB study site morphologically using the standard deviation of temporal elevation profile change with respect to average beach profiles for each transect in the study site (Larson and Kraus, 1994). Selected

transects, Transects 39 (T-39); 20 (T-20); and 2 (T-02), which represent the northern, mid, and southern sections of the study site respectively can be found in *Figure 9*. Most of the variation for T-20 and T-02 occurs at average elevations above ~-4.7 m over the 23-year study period (Figure 9D). For T-39, a DoC is not defined within the data as variability was large across the profile. *Figure 10* represents the variability of different subsections throughout the study site with the northern profiles having offshore boundaries (lower shoreface/upper offshore and upper offshore/offshore) reaching further offshore than the middle and southern profiles. This spatial difference likely contributes to the uncertainty of a DoC for T-39.

Within the active beach of all profiles, the mean elevation range of 2 to 4 meters has the largest variance in standard deviation, with the middle transect of the study area experiencing the largest variance, while the northern and southern transects are similar. Below 0 meters, T-39 once again experience the most variance while T-20 and T-02 are similar in shape with the T-20 profile being slightly more variable near mean profile elevations of -2 m.

Spatially, changes within the three selected transects are different from one another. After the initial nourishment, T-39 has a large increase in elevation across all sections within the profile (Figure 9-C). Subsequent surveys in T-39 continued to show small growth, mainly within the upper shoreface, until the Dec-01 survey where the shoreface largely increases in elevation. This increase is maintained until the Aug-08 survey where elevations in the shoreface steadily decline until the end of the survey period resulting in a duel nearshore bar.

Compared to T-39, T-20 and T-02 do not experience as much elevation change throughout the study period, yet temporal changes within the data occur over similar time periods. Following the initial nourishment, T-20 and T-02 mostly increase in the backshore and foreshore subsections. From Dec-01 to May-06, both T-20 and T-02 lost sediment within the upper offshore and offshore subsections while the nearshore bar grew seaward. After May-06, T-20 and T-02 change across the entire profile with growth in the backshore, surf zone, nearshore bar, upper offshore and offshore occurred while the channel and lower shoreface remained near the mean profile until Aug-13. The end of the study period (Jul-14-Oct-19) shows more growth in backshore, upper part of the foreshore, deepening of the channel, growth and pushing out of the nearshore bar, and loss in the upper offshore and offshore.

4.3 Volume Analysis of Beach Elevation Profiles

Total profile volumes calculated from the sum of half-cell analysis of beach profiles of the NMB study sites shows an overall increase in volume by the end of the survey period compared to the initial Jan-96 pre-nourishment survey (Figure 11). Overall, total volumes have an oscillatory pattern throughout the study period but always exceed the low volumes reflected in the pre-nourishment data calculations. The first nourishment occurred from Nov-96 to Nov-98 throughout the entire Grand Strand region, but locally, completion of the nourishment is reflected in the May-98 survey. By Apr-97, volume increased by ~1.4 $x10^6$ m^3 equating to ~70% of the volume placed at NMB. By the completion of the nourishment at NMB, the May-98 survey shows a volume change of ~1.83 $x10^6$ m^3 compared to the Jan-96 survey, ~92% of the total nourishment volume placed at NMB during the first nourishment period. Following the May-98 survey, volumes remain relatively stable until Mar-04 and May-06 during which there are large increases in volume.

The Jan-07 survey subsequently measures a decrease in volume, showing a 1.5 $x10^6$ m^3 loss of sediment from the previous year.

Following the loss of sediment from the system between May-06 and Jan-07, the second nourishment occurred between Nov-07 to Jan-09, during which time volumes increased again by approximately 0.86 $x10^6$ m^3 (based on the Jan-07 and Dec-09 surveys). This volume is ~125% greater than the amount of sediment placed at NMB. Total volume loss after the second nourishment was minimal with a loss of ~0.40 $x10^6$ m^3 between Dec-09 and Aug-15. Following Aug-15, a volume increase is calculated through the Jul-18 survey with a gain of ~1.10 $x10^6$ m^3. The Oct-18 survey shows a loss of ~0.78 $x10^6$ m^3 compared to the previous year followed by a gain of ~0.44 $x10^6$ m^3 in Oct-19. Between Jul-17 and Jun-19, two nourishments occurred, placing a total of ~0.84 $x10^6$ m^3 of material between the two events, which were interrupted by storm and hurricane events. Over the 23-year time period, the volume at NMB increased by ~2.89 $x10^6$ m^3 which is approximately ~82% of the total sediment placed from nourishments at NMB and 28% of the sediment paced within the Grand Strand throughout the study period.

Subsection volume analyses at NMB reveal that the backshore, foreshore, upper shoreface, and lower shoreface increase in volume with respect to the initial Jan-96 survey while the upper offshore and offshore overall have a decreasing trend in volume with respect to the initial survey during the study period (Figure 12). Overall, total volumes of the backshore portion of the coastal system have a positive step-like behavior over the study period with final volumes being ~1.6 $x10^6$ m^3 greater than the initial survey. Volume increases occur in the Apr-97, Nov-08, Sep-17 and the Oct-19 surveys, each following a nourishment period. The largest volume loss in the backshore subsection

occurs between the Oct-16 and Sep-17 surveys during which time Hurricane Matthew and Tropical Storm Irma impacted the coast.

Total volume increases within the foreshore range between 0.5 $x10^6$ m^3 and 0.9 $x10^6$ m^3 following the initial pre-nourishment survey, with the Jul-09 survey having the highest volume following the second nourishment. Volumes within the foreshore have an oscillatory pattern throughout the study period. The combined backshore and foreshore environments, situated above -1.2 m in elevation, account for ~ 85% of the volume increases encountered by the end of the study period.

The upper shoreface gains ~2.5 $x10^6$ m^3 in volume after the initial Jan-96 survey. Following the initial nourishment event, subsection volumes are noticed to display slight increasing trends until the Aug-15 survey, when volumes then decrease and remain steady until the end of the study period. The lower shoreface also has an oscillating pattern throughout the 23-year study period similar to the foreshore. Volumes in this subsection are ~0.4 $x10^6$ m^3 higher by the end of the study than the initial pre-nourishment value.

Volume in the upper offshore subsection was less overall than the initial Jan-96 survey with final volumes being ~ 0.2 $x10^6$ m^3 less than the first survey. Throughout the study period, the upper offshore did not continuously decrease through time but instead has an oscillatory pattern with three surveys, Apr-97, Dec-09, and Jul-14, being greater than the initial volume. The May-06 survey had the largest loss in volume after a period of storminess with a loss of ~0.3 $x10^6$ m^3 of sediment relative to the initial survey. The offshore subsection also has an oscillatory pattern with volumes being above and below the initial pre-nourishment volume throughout the study period. Volumes in the offshore

were positive between Dec-01 and May-06 surveys, during which was a period of storminess. After the stormy period between the Jan-07 and Jul-14 surveys, volumes within the offshore subsection had a decreasing trend. By the completion of the survey period in Oct-19, volumes were ~ 0.5 x10^6 m^3 less than the initial Jan-96 survey.

Correlation coefficients of total volumes are calculated to determine how the six subsections are related dynamically (Table 3). Correlation coefficients with significance values less than 0.05 are considered significant. Strong positive relationships may suggest similar effects to subsections through time while strong negative relationships may suggest the movement of sediment from one subsection to another. The highest positive correlation between subsections is between the backshore and the foreshore subsections (z = 0.87, τ = 1.59E-08), indicating that the two are strongly related and have a coupled environment. This represents the expected linkage between fair-weather and foul-weather beach profiles and equilibrizing of the nourishment fills expected for typical beach systems. Other high positive relationships are the backshore and upper shoreface (δ = 0.78, τ = 3.79E-08), and lower shoreface and upper shoreface (δ = 0.81, τ = 1.02E-06). The strongest inverse relationship is between the lower shoreface and offshore (δ = -0.77, τ = 7.54E-06). Other strong inverse relationships are the upper offshore and offshore (δ = -.07, τ = 1.29E-06), and the upper shoreface and offshore (δ = -0.50, τ = 2.04E-03). Total volume at NMB was positively related the most by the foreshore (δ = 0.72, τ = 5.88E-05) and negatively related by the upper offshore (δ = -0.56, τ = 3.82E-03).

Total volumes and volume change are calculated to determine the spatial distribution of sediment for each transect at the NMB study site (Figure 13). Figure 13-A shows a large-scale oscillation pattern across the NMB study site where

this pattern is maintained throughout the 23-year study period. Spatial volume change is in reference to the Jan-96 survey (Figure 13-B). Overall, after the initial nourishment until the end of the study period, volumes are greater than the pre-nourishment survey across the study site except at the very north and very south end of the study area. The northern profiles highlight large temporal changes for T-38 and T-39. These changes are as expected given direct morphologic influence of Hog Inlet ebb tidal delta.

Volume changes by subsection are calculated to determine spatial trends (Figure 14). The backshore subsection exhibits the step-like volume increases through time at most study sites, but the highest volume gains are measured between Transects 2-4 and 20—25; the smallest occurs between Transects 26-30 (Figure 14-A). Spatial foreshore patterns again show volume increases across the study site. Higher variability is found near the northern and southern ends of the study site which may be due to piers (green dashed lines) and outfall pipes (purple dashed lines), respectively (Figure 14-B). The upper shoreface increases in volume compared to the initial Jan-96 survey, mainly along the northern end of the study site (from T-39 to T-28, past the southern pier; Figure 14-C). Volume changes are variable across the study region's lower shoreface with volumes increasing throughout the study period except for Transects 28 and 32, where a decreasing trend is observed (Figure 14-D). The largest increase within the lower shoreface occurs along the study region's northern portion. The upper offshore lost sediment at Transects 1-25, while sedimentary changes at Transects 26-39 are more variable, mostly characterized by a more substantial sediment loss. The multibeam imaging of this region, which is discussed later, provides important, independently acquired data for interpreting the change to this area

(See Section 4.4 below). The offshore subsection volume change is unevenly distributed throughout the entire study site.

4.4 Multibeam Analysis

Multibeam bathymetry and backscatter intensity data were collected at North Myrtle Beach in March 2017, March 2018, and January 2019. The coverage includes sections of the lower shoreface-to-shelf transition zone and surveys were conducted after hurricane events (Table 2; Figure 1; Figure 15). While this analysis did not cover the same 23-year time period as the beach elevation profiles, multibeam analysis offer further insights into profile volume changes over a spatially continuous, higher spatial resolution across three subsections of interest: The lower shoreface, the upper offshore, and the offshore. This multibeam analysis builds upon the work of *Dolan (2016)*, who conducted an initial multibeam survey of much of the Grand Strand in 2015 and 2016. In the findings, *Dolan (2016)*, identified cuspate features in the shoreface-to-shelf transition zone at depths just below the 6-meter contour across many locations in the Grand Strand within the multibeam bathymetry and backscatter intensity data. Cuspate are identified in subsequent multibeam surveys showing bathymetry change (Figure 15). While there is positive and negative elevation change associated with these features, there is little to no change in position in the longshore direction. These features continue to extend across the shoreface-to-shelf transition zone with the shallow side of the cusps situated on the transition between the lower shoreface and upper offshore subsections. Sediment losses captured in bathymetric data occur in upper offshore subsection, while the offshore subsection gained sediment. Volume change between the March 2018 and March 2017 surveys quantified a loss of ~221,000 m^3. There is a gain of ~176,000 m^3 across the

overlapping survey areas between March of 2018 and January 2019. Despite the overall volume increase between March 2018 and January 2019, losses within the cuspate features occur. These losses occur where there are higher backscatter intensity values, indicating a compositional difference within the cuspate features may relate to the long-term evolution of these features.

Due to the visible minimal longshore change in cuspate locations, three longshore transects spanning the lower shoreface, upper offshore, and offshore subsections are extracted from each of the multibeam surveys (Figure 16). Cross correlation of each of the subsections are computed to determine if there is an alongshore shift associated with these features that was not identified in geotiff-based volumetric analyses (Figure 17). Correlation coefficients and lag of the greatest coefficient for each instance can be found in *Table 4*. The most significant correlation values are found in the offshore subsection where longshore shift of the bathymetry data is 0 m for the March 2017 and January 2019 analysis and the March 2018 and January 2019 analysis. A horizontal shift of +2.5 m is found between the March 2017 and March 2018 analysis. A positive shift indicates the March 2018 bathymetry dataset shifted 2.5 meters north of the March 2017 bathymetry dataset. A similar pattern is found in the upper offshore subsection. A lag of 0 m is found for the March 2017 and January 2019 analysis and March 2018 and January 2019 analysis, but the March 2017 and March 2018 data infer a +1.5 m northern shift.

The lower shoreface subsection exhibits a slightly different pattern. The March 2018- January 2019 analysis still maintains a 0 m lag, but the March 2017- January 2019 analysis resolves a northward shift of 0.5 m to the north while the March 2017-March 2018

finds a -1.5 m shift towards the south. Overall, longshore shifts are limited at for all three contour intervals.

4.5 Empirical Orthogonal Function (EOF) Analysis

EOF analysis is performed on a 23-year demeaned time series of beach elevation profiles (25 surveys) to determine temporal (PC) and spatial patterns (eigenvectors) in the cross-shore and longshore directions at NMB. Modes 1 and 2 account for the majority of the variance (>60%) and will be the focus of this study (Figure 18; Figure 19). To aid analysis, mode reconstruction of Modes one and two are performed on each survey to better visualize changes throughout the study period (Figures 20 &21). By examining cross-shore and longshore mode changes and using mode reconstruction to aid in interpretation, a comprehensive analysis of variance of elevation change at NMB could be examined for inter-annual and inter-decadal trends and their relationships to nourishments and large storm events.

Mode one accounts for ~42% of the total variability in beach profiles at NMB (Figure 18). Figure 19-A shows the Mode one eigenvectors for each transect at NMB which represents the largest spatial variability. Hot and cool colors, which represent variance of elevation about the mean profile, are inverse of one another. Larger magnitude eigenvector values explain more variance in elevation than lower magnitude eigenvector values. The first 200 meters of each transect represent similar positive eigenvector values in the longshore direction with the greatest positive values being closest to the OCRM baseline which typically lies on the crest of the primary dune. From ~250 to ~350 m offshore, mode one eigenvector values of all transects are negative and are out of phase with the first 200 m. Within this region, negative mode one eigenvector values are consistent with a net northerly longshore transport. Offshore distances greater

than 350 m vary from one another, but overall appear to mostly positive. In the longshore direction, highest positive eigenvector values further than 350 m offshore are between Transects 19 and 26. North and south of high positive area in the offshore, values are typically close to 0 which represent little variance above or below the mean. T-39 consistently shows positive eigenvector values across the profile.

Principal Components of mode one (PC 1) is found in Figure 19-B and describe the temporal variability of the mode one eigenvectors throughout the study period. Overall, PC 1 is cyclic in nature with values negative between the Jan-96 and May-06 surveys with exception to the Apr-97 survey during the first nourishment period. Following the May-06 survey, PC 1 values largely increased and remained positive until the Sep-16 survey. Subsequent surveys undulate around 0 until the end of the survey period.

In order to better understand the temporal and spatial variability in mode one throughout the study period, mode one reconstructions are performed by multiplying the M1 eigenvectors of each transect by the 25 PC1 values (Figure 20). Between Jan-96 and May-06, where PC1 values are mostly negative, reconstruction values are negative and overall increase in magnitude through time for the first ~200 meters of each transect with the exception of the Apr-97 survey which show positive but low magnitude reconstruction values in this section. In the longshore direction, reconstruction magnitudes throughout this time period are similar across the study area with the variance being in the first 50 m of each transect and around 200 meters offshore. During the same time period, ~250 to ~350 m offshore is out of phase with the onshore portion having positive eigenvalues for all transects except during the Apr-97 survey. Surveys with larger negative magnitudes on the onshore portion equate to surveys with larger positive magnitudes in the mid-section of

the study area. Higher positive magnitudes in the mid-section appear to be concentrated near the southern end of the study site. For the first 11 surveys, beyond 350 m offshore, mode one reconstruction values have positive and negative eigenvalues with smaller magnitudes in each direction.

Beginning in the Jan-07 survey until the end of the survey period, with exceptions to the Sep-17 and Jul-18 surveys, trends in each of the three sections listed above behave oppositely with mostly positive reconstruction values in first 200 m and negative eigenvector values in the ~250 to ~350 m range. The offshore section (>~350 m) continues to display variability between transects but reconstruction values are opposite in direction than earlier surveys.

Mode two accounts for ~20% of the total variability of beach profiles at the NMB study site (Figure 18). Mode two eigenvector values are more variable in the longshore direction than Mode one (Figure 19). For the first ~200 m, eigenvector values vary throughout the study area with the largest concentration of positive values between T-28 and T-33 and the largest concentration of negative values at the southern end of the study area between T-01 and T-06. Between ~175 and ~300 m offshore, values are less than zero while ~>300 m are mostly positive except the very northern most and very southernmost profiles. Positive offshore values are greatest in the northern section of the study site while decreasing in variability to the south.

PC 2 did not exhibit the same pattern as PC 1 throughout the study period. Between Jan-96 to May-06, PC 2 almost continuously decreased from positive to negative values. Beginning in the Jan-07 survey, PC 2 values increased and undulated near 0 until the Jul-14 survey. At the Jul-14 survey, PC 2 values increased slightly above 0 and then

decreased below 0 almost consistently until the end of the survey period except for the Oct-18 survey.

To understand variability in mode two throughout the study period, mode two reconstructions of each survey are performed by multiplying the M2 eigenvectors of each transect by the 25 PC 2 values (Figure 21). Like the M2 eigenvectors, three distinct regions are highlighted within the reconstructions. When PC 2 values are positive, the first ~175 m of each transect are overall positive while ~175 to ~300 m offshore values are mostly negative. Greater than 300 m offshore, values tend to be positive, with the largest magnitudes in the north and decreasing towards the south for positive PC 2 values. From Jan-96 to Mar-03, onshore and the furthest offshore sections of the profiles have positive reconstruction values that decrease in magnitude throughout this period. During this same time period, between ~200 and ~300 m offshore, eigenvector values are negative and decrease in magnitude throughout this period.

From Jan-07 to Aug-08, variance across the study area was minimal. Beginning in Nov-08, reconstruction values onshore and offshore are negative and increase in magnitude until the end of the study period except for the Jul-14 survey where values are positive. For offshore distances greater than ~300 meters, negative values extended further offshore in the northern part of the study area than the south. During this same time period, offshore distances between ~200 and ~300 m have positive eigenvector values except during the Jul-14 survey, which over increase in magnitude through the remainder of the study period. Positive eigenvector values in this mid-region are also greatest at the northern part of the study area.

5. Discussion

5.1 Wind Observations

Local wind data from June 1999 to December 2019 reveal that three distinct wind directions are dominant at the NMB study site shifting from the SW to the NE (Figure 7). Previous studies in Long Bay have found the wind patterns to be bimodal. They are controlled by seasonal patterns but dominate longshore direction here is to the southwest (Barnhardt et al, 2009; Kana et al., 2013, Weisberg and Pietrafesa, 1983; Weisberg and Pietrafesa, 1982). As our focus of study is one portion of Long Bay, it is important to address local wind field patterns and how storms impact them. Using swashes and Hog Inlet as a geomorphic indicator, *Kana et al. (2013)* found evidence bi-modal patterns within the NMB study site, with a northern component at Hog Inlet and a southern component for a majority of the study area. The Grand Strand Airport is located at the southern end of the study site and shows a dominantly NE directed winds that vary in amplitude through time (Figure 2; Figure 7; Figure 8). This may suggest this bi-modal switch of wind direction is located more southerly than previously studies. A stronger wind pattern originating from the SW may relate to the shape of the shoreline at NMB, which trends SW to NE (Figure 2). NMB lies within the mid-to-northern section of a cuspate foreland, where winds originating from the NE may be blocked by the Cape Fear headland and create highly localized effects (Figure 2).

5.2 Temporal Sediment Budget Patterns from Beach Profiles

A sediment budget using the half-cell method was established for the NMB study site (Figure 11). Total volumes largely increased throughout the study period compared to the initial Jan-96 pre-nourishment survey. Nourishment events had the largest effect on the

total volume change, with ~82% of the total nourishment volume placed, (over four successive episodes and 18 storm events) remaining within the system after the 23-year study (Figure 11; Table 1). Most of the nourishment sediment is stored within the backshore and foreshore subsections (at elevations above -1.2 m), together characterizing ~85% of the volume increase. The behavior of total volume after the first three nourishments varied from one another. After the sediment emplacement, from Nov-96 to Nov-98, total volumes did decay exponentially as expected (Willson et al., 2017). Instead, volumes continued to increase (until the Jan-07 survey), when a sudden and substantial sediment loss occurred. This increase is likely due to the movement of Hog Inlet, during which the channel and growth of the ebb-tidal delta was directly influencing upper and lower shoreface elevations, therefore volumes, along the northern end of the study site (Figure 22). Data from Transect 39 best illustrates the growth of the ebb-tidal delta during this time period where large increases in elevation, mostly within the upper shoreface, are measured (Figure 9).

While not as impactful as nourishment events, stormy periods have visible impact on total volume changes throughout the study period. Tropical storms and hurricanes are frequent following initial volume placement, from where materials moved parallel to the coast, favoring onshore transport of sediment (Figure3; Table 2). During this stormy period (1999-2006), volumes in the offshore subsection also increase, but these sediments may have derived from the lower shoreface or upper offshore, given that correlation values with the offshore are strongly negative (δ = -0.77 and δ = -0.75, respectively). For Long Bay, the frequency, magnitude, and duration of atmospheric patterns play a large roll in sediment dispersal pattern (Warner et al., 2012). The sudden loss of sediment in Jan-07 is likely due

to the cessation of large storm events that may have been supplying sediment; beach thus rapidly returning to an equilibrium with lower intensity ENE winds (Figure 8; Table 1).

Total volumes decay after the second nourishment event, as expected; however, it appears that no long-term equilibrium was attained as volume estimates do not reach pre-nourishment values (Willson et al., 2017). This may be due to the increase in storm events beginning in 2015, which persists until the end of the survey period. The increase in storminess in 2015 results in an increase in total volume before the third nourishment. Following the third nourishment, volumes once again decline substantially. This decline may relate to Hurricane Florence, which made landfall in Wrightsville Beach, NC, situated only ~100 km north of the study site. The path of Hurricane Florence differed from previous hurricane tracks (Figure 3). Instead of traveling up the coast, Hurricane Florence came directly perpendicular to the shoreline with the front right quadrant impacting Wrightsville Beach by pushing water onshore; the front left quadrant impacting NMB by pushing water offshore., This would likely lower wave base and possibly moving sediment offshore (onto the shelf), beyond our study area boundaries (Figure 3).

Volumetric changes are not evenly distributed throughout the study area. Subsection volume analyses determine that the backshore, foreshore, upper shoreface, and lower shoreface mostly gain sediment throughout the study period while the upper offshore and offshore subsections mostly lost in overall volume (Figure 12). Changes in these subsections appear to highly impact beach nourishment events and/or stormy periods (Table 1; Table 2). As nourishment sediments are placed on the upper beach, they disperse throughout the active beach overtime by wave processes (Willson et al., 2017). The backshore and foreshore subsections reflect the addition of sediment during the

nourishment events and have a step-like pattern through time with the backshore subsection after nourishment. Aside from the initial nourishment, upper shoreface does not have large increases in volume following nourishment events, unlike the backshore and foreshore. Instead, it slowly receives sediment throughout much of the study period. This is because nourishment sands move slowly to fill in the accommodation space likely from background loss from the upper beach or due to onshore transport.

The lower shoreface is influenced by both nourishment and periods of large storm events. Following nourishment placement, volumes in the lower shoreface increase from the distribution of nourishment sediments but decrease during stormy periods given the lowering of wave base. The upper offshore subsection is slightly influenced from nourishment events, but overall, more affected by large storms and the therewith associated base-level lowering. The offshore subsection is inversely related to the other subsections (Table 3). While offshore volume changes recorded a net loss (compared to the initial pre-nourishment survey), the offshore exhibits short-loved gains throughout the study period. A period of positive volumes is observed between Sep-99 and May-06, relating to heightened storm activity; this was followed by the sudden loss of sediment after the cessation of frequent storm events. Volume increases during the period of storminess likely related to the movement of sediment from other subsections (e.g. lower shoreface and upper offshore), where strong inverse relationships are found to the offshore. Total volumes increased overall during this period of storminess; however, only the offshore subsection experiences large positive gains during this time. This volume increase probably relates to the onshore push of sediment from the shelf by storms trending from SW to NE (Figure 3; Figure 22). In Jan-07, volumes quickly decrease as sediment from this subsection

likely moved into the upper offshore and lower shoreface subsections during fair weather conditions.

5.3 Spatial Sediment Budget Patterns from Beach Profiles

The three beach profiles examined reveal differences in geomorphology across the study site (Figure 9). Of the three selected profiles (T-39, T-20, and T-02), mean profile elevations greater than 0 m exhibit the large range of variance which is the result of sediment placement from multiple large-scale nourishments, typically placed above MLW with a constructed "toe of the fill" extending to native slope landward of the surf zone (~-1m). Mean profile elevations less than 0 m show a decrease in temporal variance from north (T-39) to south (T-02; Figures 9-D and 10). Variability is related to proximity to Hog Inlet, 0.5 km north of T-39, and adjustments associated with its sedimentary dynamics (e.g., changes in channel and bar configurations). Another factor is sediment dispersal across adjacent beach systems. T-39 can be used as a proxy to reflect the movement of the ebb tidal delta of Hog Inlet throughout the study period, specifically within the upper and lower shoreface as they vary in elevation and in time than that of T-20 and T-02.

Volumes within the upper and lower shoreface subsections at Hog Inlet continue to increase after the initial nourishment, peaking in Mar-04 and remaining high until Aug-08. During this time period, the channel and ebb-tidal delta of Hog Inlet was closest to the northern end of the survey area, delivering sediment and causing growth at T-39 (Figure 22 A, B, and C). Volumes at Hog Inlet then decrease, to elevations of the Jan-96 survey. This is likely related to the movement of the channel and a northward shift of the ebb-tidal delta (Figure 22 D, E, and F). While volumes at Hog Inlet began to decrease at these subsections, the upper and lower shoreface across the remainder of the study site began to

increase. This increase was spatiotemporally uneven; T-02 did not experience as much growth as T-20. Frequent storm events in the 2000's may have influenced changes to the inlet, document in elevation profiles and aerial photography (Figure 22*)*. Profile analysis shows that stormy periods (1999-2006 and 2015-2019) seem to affect both T-05 and T-00, as upper offshore and offshore sections of the profiles document sediment losses while the nearshore bar grew and moved seaward (Figure 9). Although longshore currents tend to change seasonally at this study site, *Aubrey and Speer (1984)* found that inlets can migrate in the updrift direction during stormy periods, specifically after a storm breach.

The longshore extent of the inlet can be best examined in spatial subsection volume distribution (Figure 14). Within the upper and lower shoreface subsections, the southern extend of the inlet is near T-28, south of the southern pier. The increase in volume may be due the combination of both piers which could create a groin like setup and inhibit sediment flow, trapping sediment between the two piers. The southern longshore extent of Hog Inlet, recognized in the spatial volume analysis, exceeds that of the SC Department of Health and Environmental Control (DHEC) definition of an inlet erosion zone baseline (Figure 23). *Section 48-39-270* of th*e Title 48-Environmental Protection and Conservation Chapter 39 Coastal Tidelands and Wetlands* from the *South Carolina Code of Laws* defines an inlet erosion zone as:

> *"…a segment of shoreline along or adjacent to tidal inlets which is influenced directly by the inlet and its associated shoals."*

Figure 23 shows the SC DHEC definition of an inlet erosion zone for Hog Inlet. This zone on the NMB side of the inlet only reaches that of T-39. While changes within

the shoreline may not be influenced beyond this transect by Hog Inlet, changes within the lower subsections reach beyond this point, even at inter-annual time scales.

In addition to Hog Inlet and the influence of the piers, spatial subsection analysis also finds outfall pipes influences volume changes through time by inhibiting sediment flow in the alongshore direction and potentially causing scouring on the downdrift side. The outfall pipes extend to the shoreface-to-shelf transition zone and may also behave as a groin field in deeper waters.

5.4 Empirical Orthogonal Function Analysis

While eigenvectors represent variance from the mean, they *may* be attributed to physical processes or events. Mode one likely represents nourishments events and the distribution of sediments following these sudden elevation fluxes. Mode one eigenvectors represent two areas of high elevation changes with opposing directions. These areas are the backshore to the lower shoreface (0 to ~200 m cross-shore) and the shoreface-to-shelf transition zone (~250 to ~350 m cross-shore). By comparing subsection volume analysis to mode one eigenvectors, it is determined that this mode could represent a physical process. Periods of volume increase on the upper portions of the beach profile relate to loss in the upper offshore subsection (Figure 19). The redistribution of the nourishment sediment is related to regular wave processes and storm events. As beach nourishment sediment is placed on the backshore and foreshore subsections, sediment moves into the surf zone and into alongshore transport due to wave activity returning the beach to a more typical “equilibrium” profile related to the steep slopes the fill is constructed to conform to. During periods of storminess from 1999-2006 and 2015-2019, the variance within the upper and lower portion of the beach profiles increases. PC1 follows an oscillatory pattern

in time that relates to these storm events. Mode one represents ~42% of the total variance within the beach elevation profiles. Typically, longshore transport is considered to be one of the main controls of sediment budgets (Fredsoe and Deigaard, 1992) but *Park, Gayes, and Wells (2009),* and *Barnhardt et al. (2009)* found cross-shore transport to be dominant within the Grand Strand to enable sediment budgets to be balance relative to the long term erosion rates of the region. EOF analysis of beach elevation profiles find that mode one supports cross-shore transport occurring after the placement of beach nourishment sediment and intensifies during period of storminess.

Mode two, which represents ~20% of the total variance, likely does not represent one physical processes. Opposing elevation relationships within the M2 eigenvector are observed in the upper offshore/offshore regions (~>250 m cross-shore distance), with variability increasing towards the north, and the upper shoreface region (~175 to ~250 m cross-shore). The tapering of the offshore variance to the south is likely due to the influence of Hog Inlet. Changes in Hog Inlet, observed by T-39 in *Figure 9* and aerial photography in *Figure 22*, coincide with changes in this upper offshore/offshore region.

Periods of little change in the growth of Hog Inlet in T-39, specifically the Jan-07, May-08, and Aug-08 surveys, show little variability in the inlet in the cross-shore direction and is represented by little to no variance within mode two. Using subsection volume change, we have determined the approximate southern longshore extend of the influence of the inlet is approximately near T-28, just south of the southern pier. This same pattern is recognized within mode two with higher variability in elevation also associated between the piers. As patterns within mode two match temporal and spatial trends associated with Hog Inlet, mode two may be a good representation of variance occurring throughout the

study area due to inlet changes. While the inlet extent appears to end near T-28, mode two shows evidence that it's southern longshore extent may extend further south then what is recognized within the half-cell volume analysis. As discussed in section 5.2, profiles examined show a longshore trend within the upper and lower shoreface in which the magnitude increases to the south that may be related to changes in inlet dynamics. In addition to spatial volume analysis, EOF analysis, which shows the variability in beach profile data, also challenges the current definition of an inlet erosion zone that is characterized by SC DHEC. This result should be considered for future analysis and by coastal managers.

The southern end of the study site displays a trend in the offshore different from the rest of the profiles. This inverse relationship may be due to the influence of all three outfall pipes, which is also observed in sub suctional volume changes, and/or the influence of White Point Swash, located directly south of T-01, and/or an edge effect of nourishment volume leaving the study area as this is terminus of the NMB nourishment projects. Unlike that of T-39, profile analysis did not find effects from White Point Swash, especially within the upper or lower shoreface, likely due to the much smaller size of the swash system. Instead, elevation profile variance at the southern end of the study site is smaller than mid or northern sites (Figure 9-D).

In addition to inlet processes and the longshore effect of piers and groins, mode two may also represent seasonal patterns of a 'winter' or 'summer' profiles. Typically, to capture a clear seasonal trend, surveys should be taken at even increments multiple times a year. For example, *Short et al. (2014)* has monthly profile surveys over a six-year period to clearly extract seasonal trends and magnitude changes. Surveys for this study were taken

at various points during the year and would not clearly reflect seasonal changes as highlighted in other EOF studies but are likely to still exist. During fair weather typically associated with the summer period, the berm builds and becomes wide and flat. During the periods of heightened wave energy, the berm is eroded and removed from the beach into the near shore bar system and shoreface, causing a steeper profile. This inverse relationship is also observed in mode two within the backshore and upper shoreface. Overall, PC 2 decreases in elevation variance after the initial nourishment until Mar-04 where elevation variance increases again, but in the opposite direction, until the end of the first period of storminess in May-06. Following that, elevation variance decreases again until the beginning of the second stormy period where the elevation variance continues to decrease until the end of the survey period. While mode two may represent more than one physical process, the changing of the inlet likely is the most dominant driver for variance within the beach profiles, especially the northern third of the study area, and elsewhere the interplay of timing of nourishment and storms is evident.

5.5 Lower Shoreface-Shelf Transition Zone

Defining the DoC by standard deviation of the beach profile envelops at the NMB study site (~-4.7m) closely aligned with *Kana, Kaczkowski, and McKee, 2011*, who found the DoC for Myrtle Beach, located directly south of the NMB study site, to be ~-4.6 m NGVD (~-4.8 NAVD) for beach profiles collected from 1987 to 2011. Typically, sediment displaced below the depth of closure is considered to be a loss to the system over shorter time periods (Morang and Birkemeier, 2005). Over the study period, volume changes larger than the calculated depth of closure is apparent. In addition to the cross-shore transport

highlighted in the EOF analysis in Section 5.4, multibeam analysis within this transition zone spatially shows changes not observed in beach profile data.

Cuspate features in the lower shoreface-to-shelf-transition zone, first identified by *Dolan, 2016,* and now in subsequent multibeam surveys, show a better spatial resolution of processes occurring at the lower elevation subsections. Bathymetry differences show little to no longshore position change within these features. To verify if these features are not shifting, a cross-correlation is performed at three different contour intervals within this zone, but little change was determined (Figure 17). While there is little longshore position change, volume change within these features is evident. Overall, the cuspate features have volume loss in areas with coarser texture and volume gain in areas with finer texture even when total volume change may increase or decrease (Figure 16). This textural differences is likely due to the location of these features eroding into stratigraphic boundaries (Dolan, 2016) and was suggested by *Dolan, 2016* to have a similar formation like that of sorted bedforms (a.k.a. ripple-scour depressions; Cacchione et al., 1984 now referred to as transverse bedforms) developing from self-organizing feedback between relief, sediment texture (roughness) and flows (Murray and Thieler, 2004). Sub sectional volume analysis shows the upper offshore lose more sediment during frequent storm periods due to the lowering of wave base during which maintenance of these features may occur. Multibeam data, following significant storm events, continues to show the scarping of the features liberating sediment that may be added to the sediment budget. While much about these features is unknown, they may be a sediment source for the NMB study area in addition to the large-scale nourishments.

6. Conclusion

This work characterized inter-annual and inter-decadal trends of beach elevations at North Myrtle Beach, South Carolina, by analyzing a unique long-time series of beach profiles and a series of very shallow water multibeam imagery of the lower shoreface region during a stormy period. Throughout the period of study, the area was impacted by a series of beach nourishments that contribute large volumes of sediment to the upper elevations of the system (above MLW), which adjust to the unnaturally steep slopes of the construction over typical day to day and seasonal changes in waves and currents as well as two distinct periods of heightened storm activity that impacted the area. Spatially, the system is influenced by a large tidal inlet at the northern system boundary and, locally, two large shore perpendicular piers in the northern portion of the area as well as a series of smaller storm water outfall pipes. The latter provide smaller disruptions to sediment dispersal.

The beach profiles were analyzed using traditional analyses and half-cell volume calculations for overall volume change of the system and means of tracking efficacy of beach nourishment projects. EOF analysis is an important tool for understanding spatial and temporal patterns in both cross-shore and longshore data analysis that may highlight trends that are not as readily quantified from traditional profile analyses. While EOF modes may not represent physical processes, they can be extremely useful for identifying patterns throughout time and can be interpreted in terms of known spatial and temporal influences of nourishment, morphologic features, engineering structures, and wind and storm processes.

Half-cell calculations show an overall increase in volume throughout the study period experiencing large positive jumps due to nourishment events with ~85% of the remaining nourishment volume being maintained within the backshore and foreshore. Subsections at NMB are variable throughout the study period, but overall maintain a positive or negative oscillatory trend throughout time. While not as drastic, periods of frequent storm events directly affect total volume changes, most evidently in the lower shoreface, upper offshore, and offshore subsections. This is probably because of where wave base is typically lowered. Overall, these subsection patterns are consistent across most transects in NMB, which suggests an overall uniform change in morphology for the study area, except for the northern end of the study site. This is where geomorphology is largely controlled by Hog Inlet, best captured by the northern-most transect but the longshore influence across the study side can be found in subsectional volume and EOF analyses. Fluctuations within the inlet may be related to periods of large storm events and sediment changes from the ebb-tidal delta. Changes in the ebb-tidal delta may redistribute sediment across the study site that is not fully lost to the system. Multibeam analysis suggests that cuspate features in the lower shoreface to offshore transition zone may be a source of sediment contributing to the sediment budget. While the formation of these features is unknown, their location on stratigraphic units and similarity to sorted bedforms may provide a future area of exploration.

EOF analysis was performed to determine cross-shore and longshore variance of beach profile elevations over the 23-year study period. Two modes, which collectively represent ~62% of the total variance, displayed evidence of cross-shore and longshore transport. Mode one best reflected nourishment events and the distribution of nourishment sediment

through time. Mode two appears to be most related to changes within Hog Inlet that affect larger regions of the study area than previously thought. Mode two also highlights the impact of piers and outfall pipes to the variance within the data and possibly seasonal changes.

Using a combination of methods, like half-cell calculations and EOF analysis, various inter-decal trends, and their relation to nourishment and storm events, are examined for the North Myrtle Beach study area. These trends can be useful for beach managers and modelers alike to best understand the local coastal system. To better understand the effects of nourishments and storm events, higher spatial resolution datasets, like LiDAR drone imagery and additional multibeam sonar of the continental shelf throughout time would facilitate a better understanding sediment transport. While much was learned about Hog Inlet during this evaluation, a sediment budget of the inlet and associated ebb-tidal delta could also provide a better understanding of the amount of nourishment sediment captured by the inlet and its long-term response to storm events.

7. Tables

Table 1: Nourishment dates and volume placement

Nourishment #	Start Date	End Date	NMB Placement	Grand Strand Totals*
Nourishment 1	Nov-96	Nov-98	1,987,800 m^3	4,816,620 m^3
Nourishment 2	Nov-07	Jan-09	688,100 m^3	2,484,732 m^3
Nourishment 3	Jul-17	Nov-17	382,000 m^3	1,146,500 m^3
Nourishment 4	Jun-18	Jun-19	458,700 m^3	2,000,000 m^3
Total			3,516,600 m^3	10,447,852 m^3

*Grand Strand totals includes Surfside Beach, Garden City Beach, Myrtle Beach, and North Myrtle Beach

Table 2: North Myrtle Beach surveys and major tropical storm/hurricane (TS/H) events. Event date is the actual date of the event while the event date shortened is how the dates will be referred to in the document.

Event	Event Date	Event Date Shortened
Survey-1	1/23/1996	Jan-96
Survey-2	4/5/1997	Apr-97
Survey-3	5/22/1998	May-98
Survey-4	3/24/1999	Mar-99
TS Floyd	9/15/1999	Sep-99
Survey-5	9/23/1999	Sep-99
Survey-6	10/14/2000	Oct-00
Survey-7	12/4/2001	Dec-01
H Kyle	10/11/2002	Oct-02
Survey-8	3/24/2003	Mar-03
H #7	7/25/2003	Jul-03
Survey-9	3/5/2004	Mar-04
H Charley	8/14/2004	Aug-04
H Gaston	8/29/2004	Aug-04
TS Frances	9/6/2004	Sep-04
TS Jeanne	9/27/2004	Sep-04
Survey-10	5/11/2005	May-05
TS Tammy	10/5/2005	Oct-05
Survey-11	5/4/2006	May-06
TS Alberto	6/13/2006	Jun-06
Survey-12	1/31/2007	Jan-07
Survey-13	5/16/2008	May-08
Survey-14	8/12/2008	Aug-08
Survey-15	11/11/2008	Nov-08
Survey-16	7/10/2009	Jul-09
Survey-17	12/5/2009	Dec-09
Survey-18	8/13/2013	Aug-13
Survey-19	7/23/2014	Jul-14
Survey-20	8/28/2015	Aug-15
H Joaquin	10/4/2015	Oct-15
H Bonnie	5/29/2016	May-16
TS Colin	6/6/2016	Jun-16
TS Hermine	9/1/2016	Sep-16
TS Julia	9/14/2016	Sep-16
Survey-21	10/4/2016	Oct-16
H Matthew	10/7/2016	Oct-16
TS Irma	9/10/2017	Sep-17
Survey-22	9/21/2017	Sep-17
Survey-23	7/20/2018	Jul-18
H Florence	9/14/2018	Sep-18
Survey-24	10/6/2018	Oct-18
H Dorian	9/5/2019	Sep-19
Survey-25	10/18/2019	Oct-19

Table 3: Correlation coefficients and significant values for subsection volume analysis at NMB.BS =Backshore, FS = Foreshore, US =Upper Shoreface, LS = Lower Shoreface, UO = Upper Offshore, O = Offshore, and T = Total Half-Cell Volume. Red correlation coefficient numbers indicate a positive relationship and blue correlation coefficient numbers indicate negative relationships. Darker colors represent a greater relationship than lighter colors. Values are considered significant if they are less than 0.05.

NMB Correlation Coefficients							
	BS	**FS**	**US**	**LS**	**UO**	**O**	**T**
BS	-	0.87	0.78	0.71	-	-0.50	0.66
FS	0.87	-	0.80	0.59	-	-0.39	0.72
US	0.78	0.80	-	0.81	-	-0.59	0.55
LS	0.71	0.59	0.81	-	0.44	-0.77	-
UO	-	-	-	0.44	-	-0.75	-0.56
O	-0.50	-0.39	-0.59	-0.77	-0.75	-	-
T	0.66	0.72	0.55	-	-0.56	-	-

NMB Significance Values							
	BS	**FS**	**US**	**LS**	**UO**	**U**	**T**
BS	-	$1.59x10^{-8}$	$3.79x10^{-6}$	$7.41x10^{-5}$	–	$1.16x10^{-2}$	$6.94x10^{-4}$
FS	$1.59x10^{-8}$	-	$1.45x10^{-6}$	$1.95x10^{-3}$	–	$5.30x10^{-2}$	$1.11x10^{-4}$
US	$3.79x10^{-6}$	$1.45x10^{-6}$	-	$1.02x10^{-6}$	–	$2.04x10^{-3}$	$4.71x10^{-3}$
LS	$7.41x10^{-5}$	$1.95x10^{-3}$	$1.02x10^{-6}$	-	$2.76x10^{-2}$	$7.54x10^{-6}$	–
UO	–	–	–	$2.76x10^{-2}$	-	$1.29x10^{-5}$	$4.29x10^{-3}$
O	$1.16x10^{-2}$	$5.30x10^{-2}$	$2.04x10^{-3}$	$7.54x10^{-6}$	$1.29x10^{-5}$	-	–
T	$6.94x10^{-4}$	$1.11x10^{-4}$	$4.71x10^{-3}$	–	$4.29x10^{-3}$	–	-

Table 4: Cross-correlation values and lag (m) for multibeam cross-sections

Lower Shoreface (-4 to -5 m)	**Correlation Coefficient**	**Lag (m)**
March 2017 & January 2019	0.60	0.5
March 2018 & January 2019	0.50	0
March 2017 & March 2018	0.48	-1.5
Upper Offshore (-5 to -6 m)	**Correlation Coefficient**	**Lag (m)**
March 2017 & January 2019	0.36	0
March 2018 & January 2019	0.47	0
March 2017 & March 2018	0.54	1.5
Offshore (-6 to -7 m)	**Correlation Coefficient**	**Lag (m)**
March 2017 & January 2019	0.69	0
March 2018 & January 2019	0.67	0
March 2017 & March 2018	0.68	2.5

8. Figures

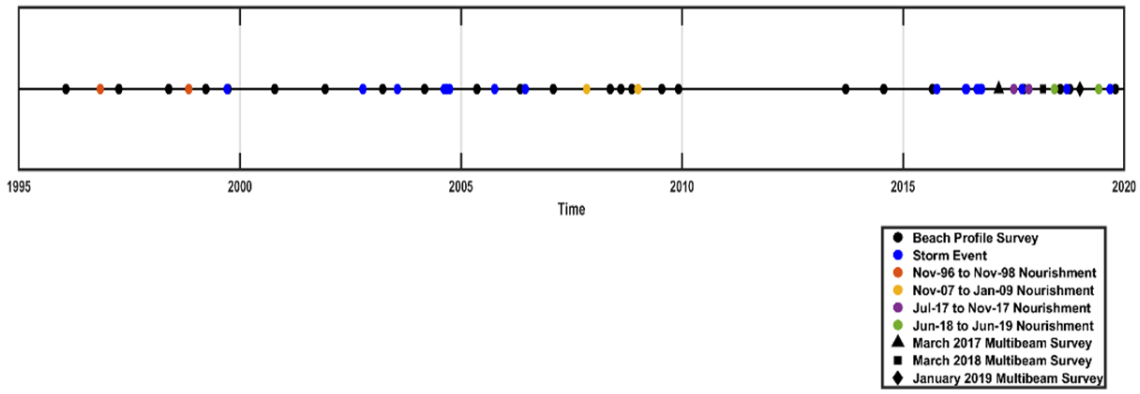

Figure 1:Timeline of events for this study. Names of storm events and specific survey dates can be found in Table 2.

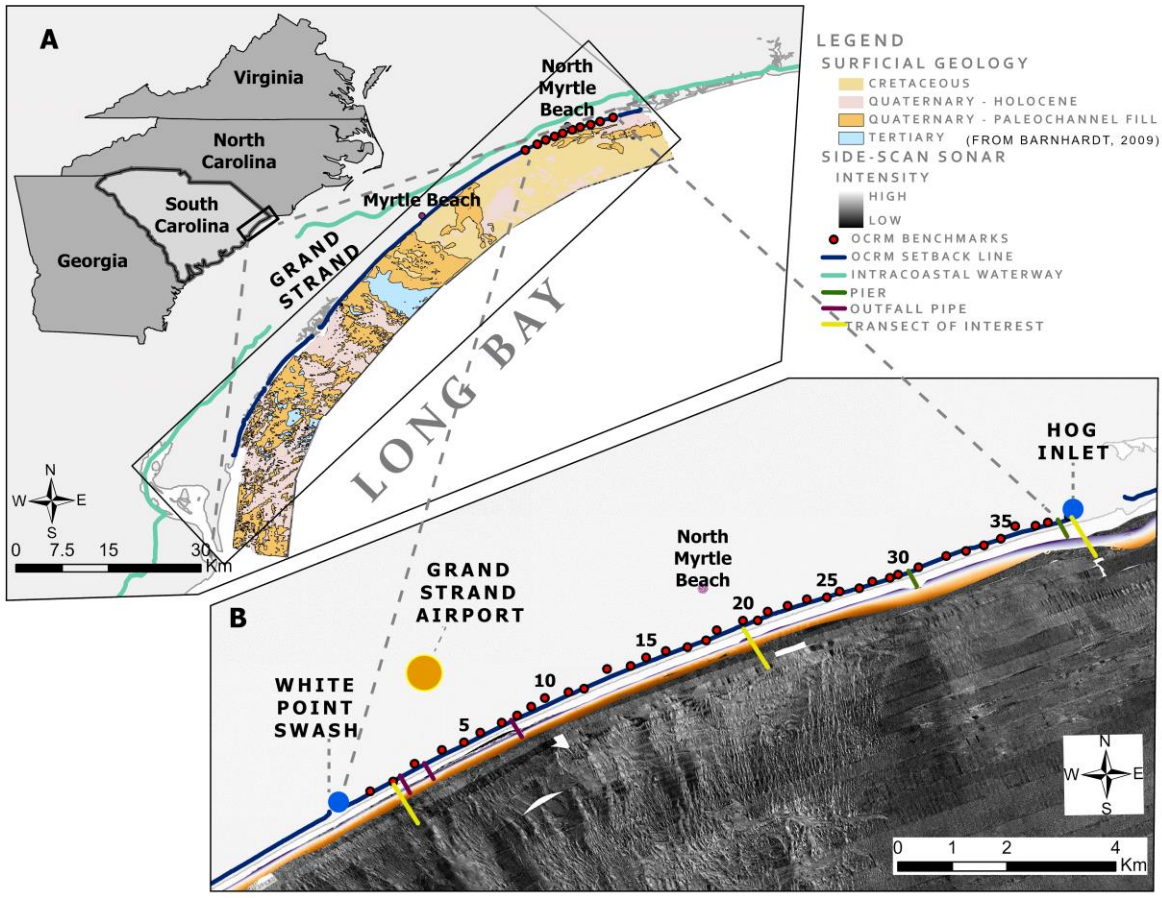

Figure 2: (A) Location of the Grand Strand with surficial geology from the USGS Coastal Erosion Study (Barnhardt, 2009); (B) North Myrtle Beach study area with side-scan sonar coverage (Barnhardt, 2009). Red circles represent the 39 OCRM transects analyzed in this study. The three transects of interest, T-02, T-20, and T-39 are represented by yellow lines. Outfall pipes are represented as purple lines and piers are represented as green lines. Yellow circle represents the Grand Strand Airport where local wind data is collected by NOAA.

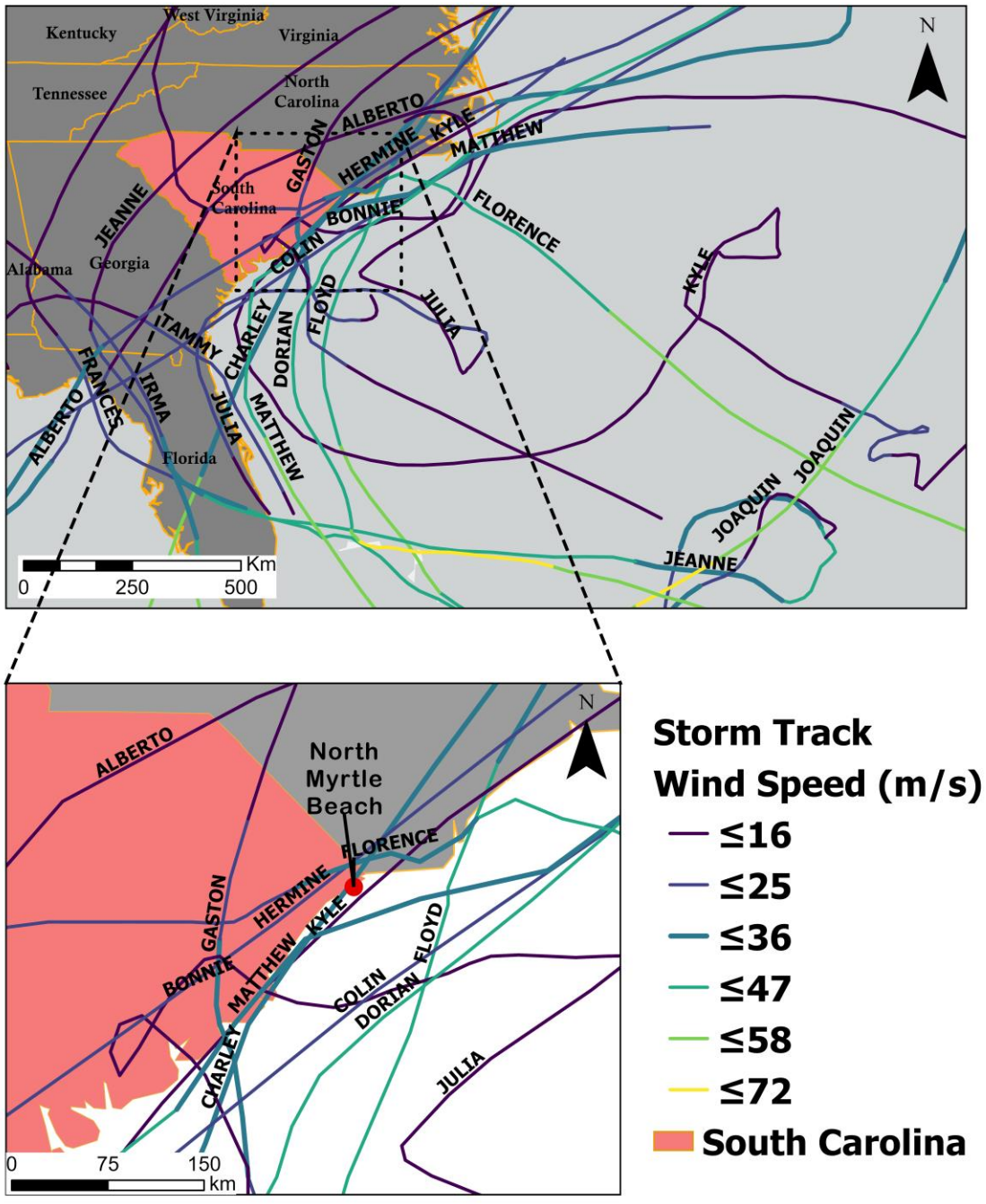

Figure 3: Hurricane and tropical storm tracks where the color of the track indicates wind speed (m/s) (see legend).

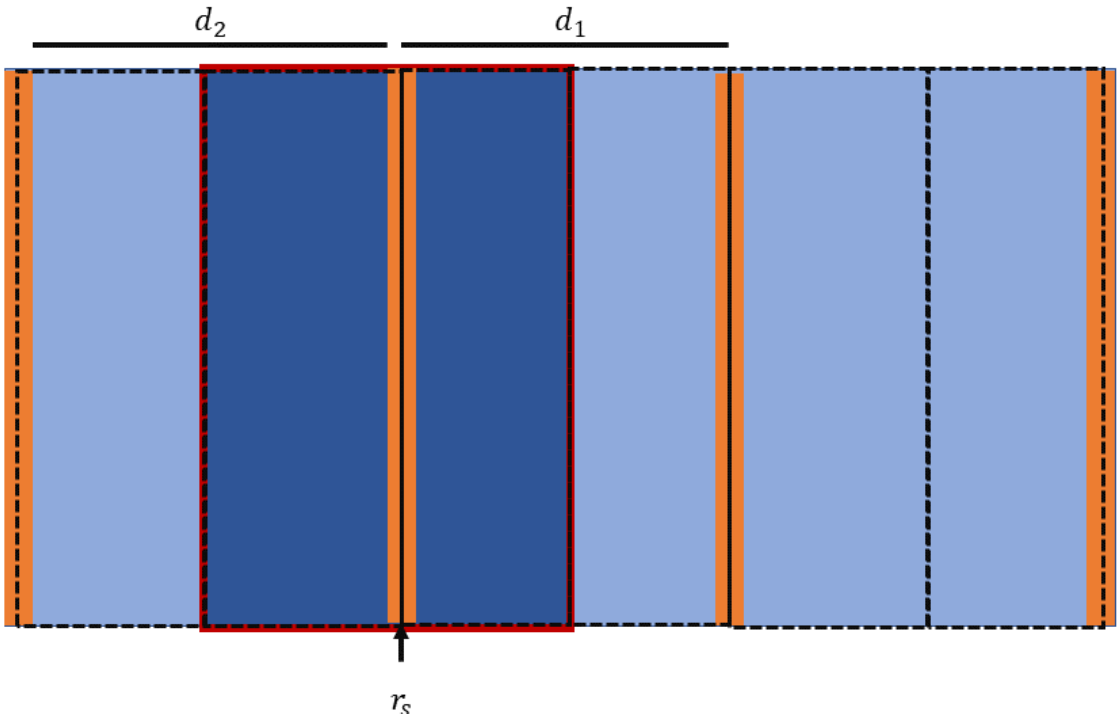

Figure 4: Visual representation of the half-cell volume. Volumes of each transect (r_s), represented by orange lines, are multiplied by half the distance to their adjacent profiles to get a total volume represented by that transect (dark blue rectangle). A total of all transects volume represent the total volume for the study area.

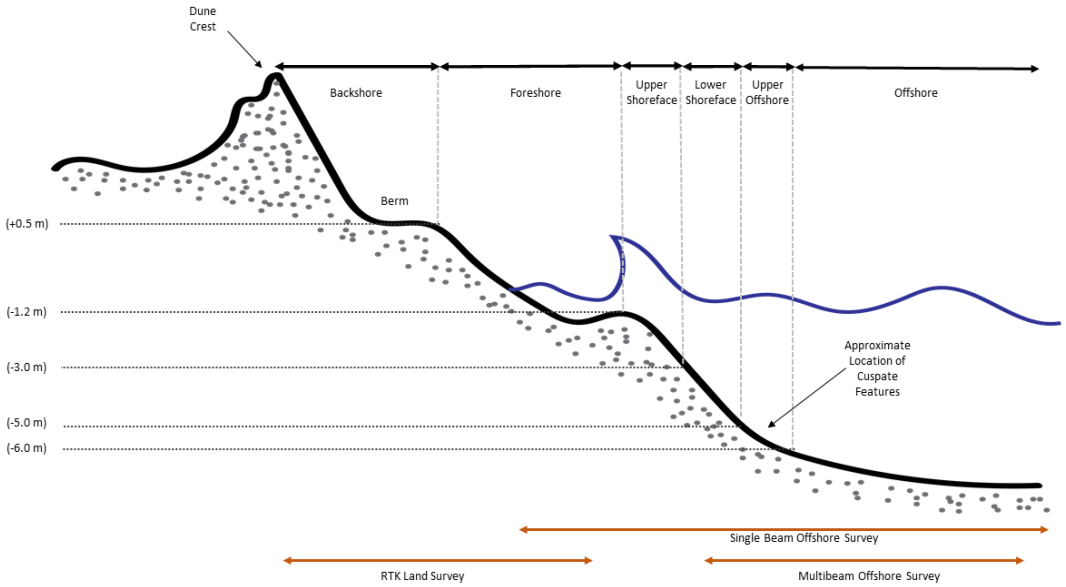

Figure 5: Elevation contour levels (m), refenced to NAVD88, distinguishing the subsections analyzed in this study. Subsections represent the backshore, foreshore, upper shoreface, lower shoreface, upper offshore, and offshore morphological boundaries. Orange arrows represent the approximate cross-shore distance of each of the three survey techniques. Figure adapted from Park, Gayes, and Wells (2009).

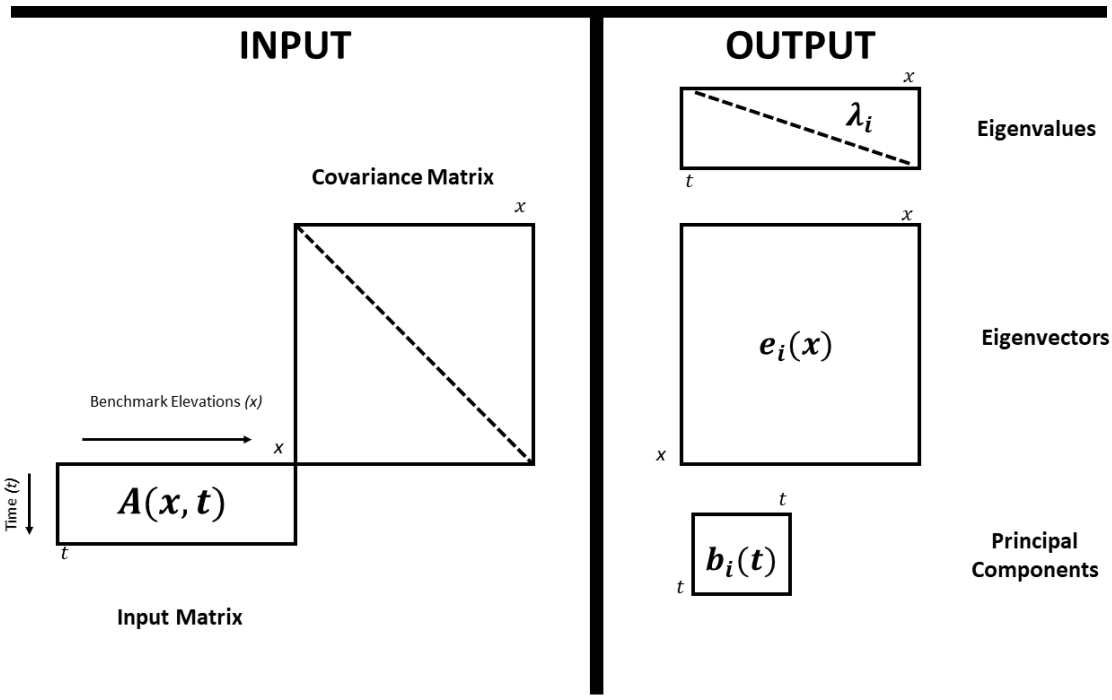

Figure 6:Set up of data matrix used in the EOF analysis. Figure adapted from Baldwin (2008).

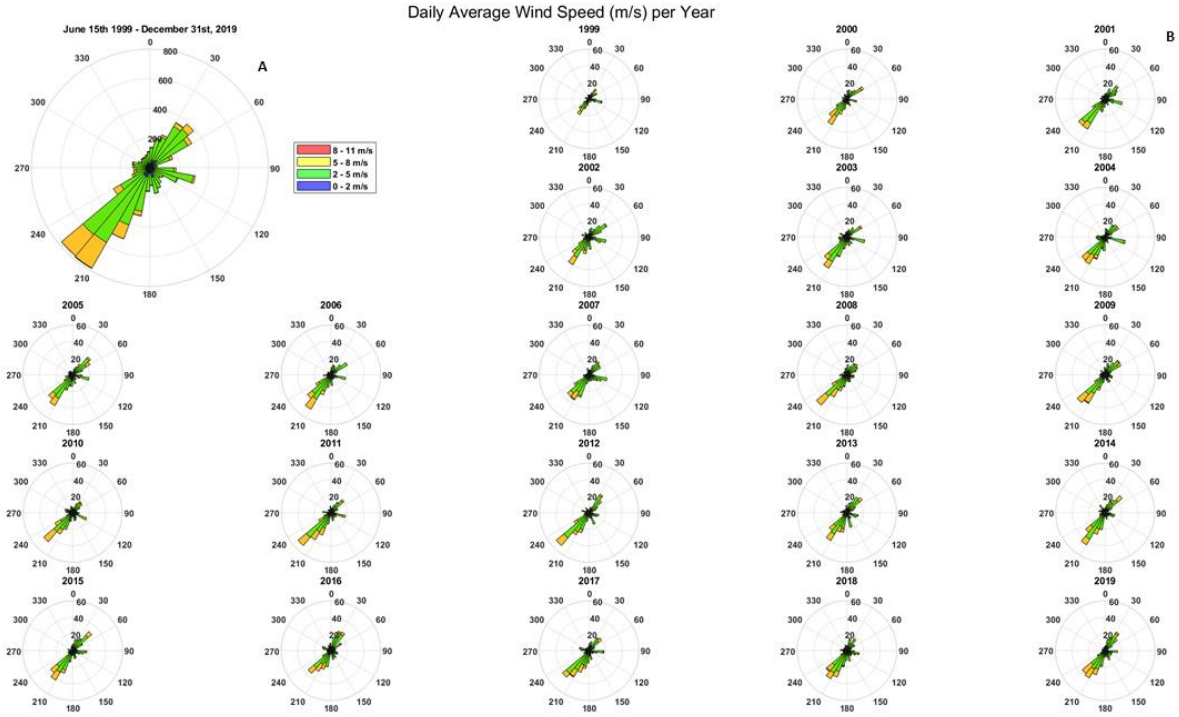

Figure 7:Wind rose diagrams for North Myrtle Beach Airport showing daily average wind speeds and direction.

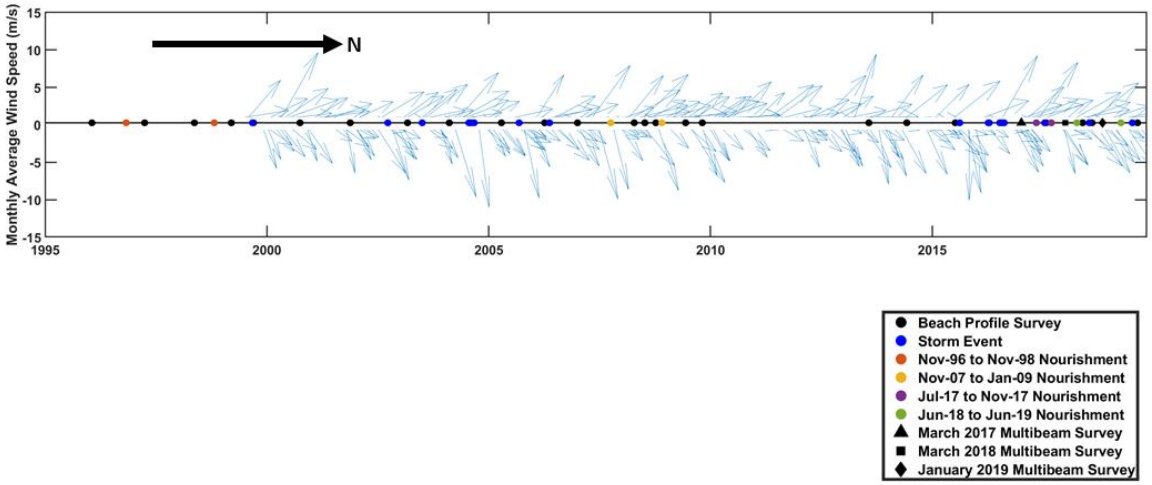

Figure 8: Monthly wind speed averages (m/s) taken from the Grand Strand Airport in North Myrtle Beach, SC representing the direction towards which the wind is blowing. The 0 m/s axis represents the timeline of events found in Figure 1.

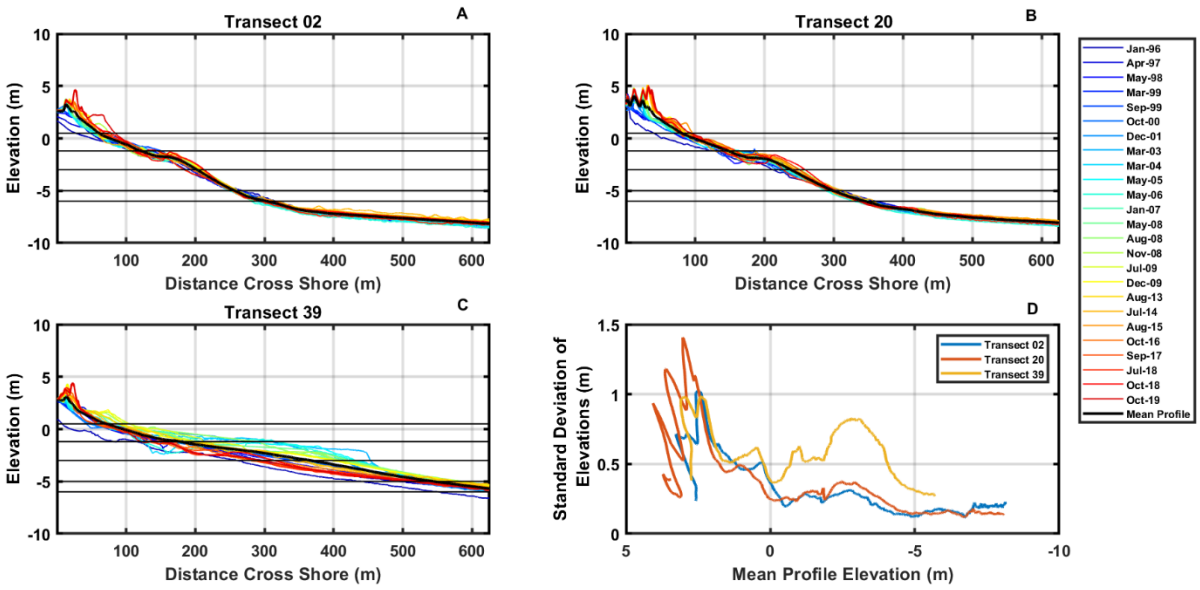

Figure 9: Beach elevations profiles of Transect (A) 02, (B) 20, and (C) 39 representing the southern, mid, and northern sections of the study area respectively (Figure 2). Black horizonal lines represent subsections analyzed in this study (Figure 5). Standard deviations with respect to mean beach profiles of Transects 2, 20, and 39 can be found in D

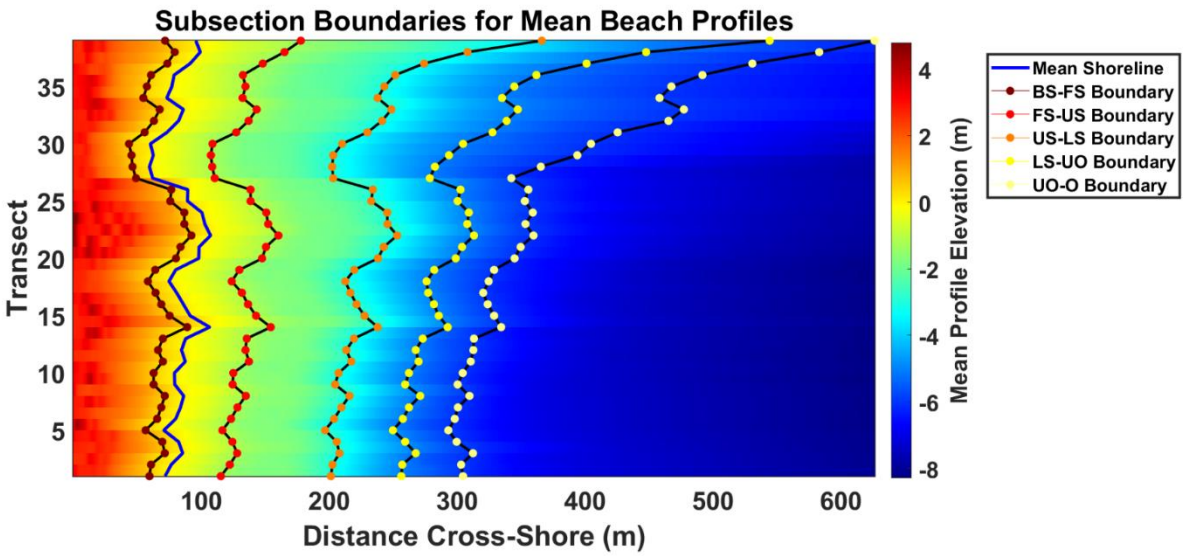

Figure 10: Mean beach profiles with subsection boundaries: the backshore (BS; z >0.5 m), foreshore (FS; 0.5 m < z ≤ -1.2 m), upper shoreface (US; -1.2 m < z ≤ -3 m), lower shoreface (LS; -3 m < z ≤ -5 m), upper offshore (UO; -5 m < z ≤ -6 m), and offshore (O; z < -6 m) highlighting the longshore variability.

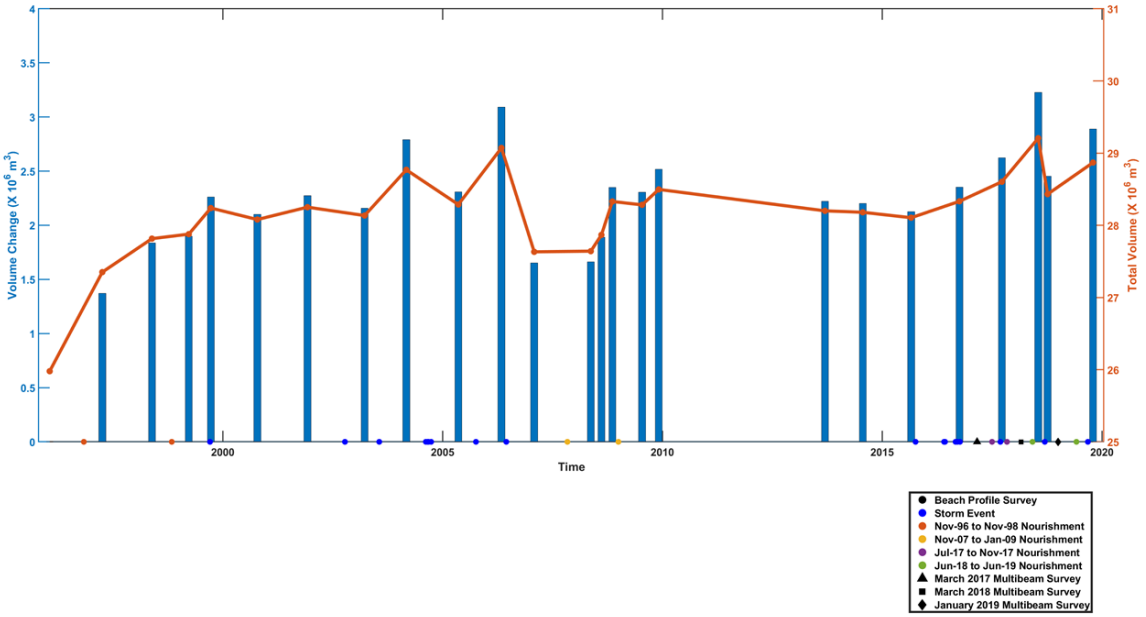

Figure 11: Total half-cell volume and volume change for NMB through the survey period. Volume change is relative to the initial Jan-96 pre-nourishment survey. Timeline of events can be found in on the x-axis.

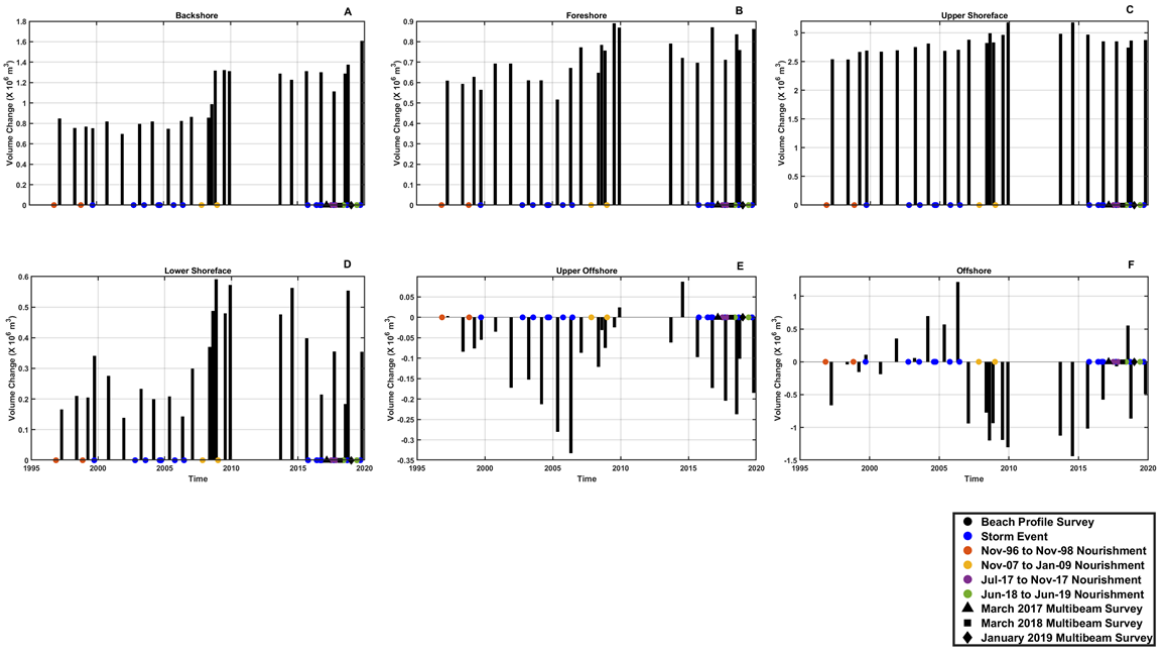

Figure 12: Half-cell volume change at each subsection for NMB through the study period relative to the initial Jan-96 pre-nourishment survey (A-F). Timeline of events can be found on the 0 m³ axis of each subsection.

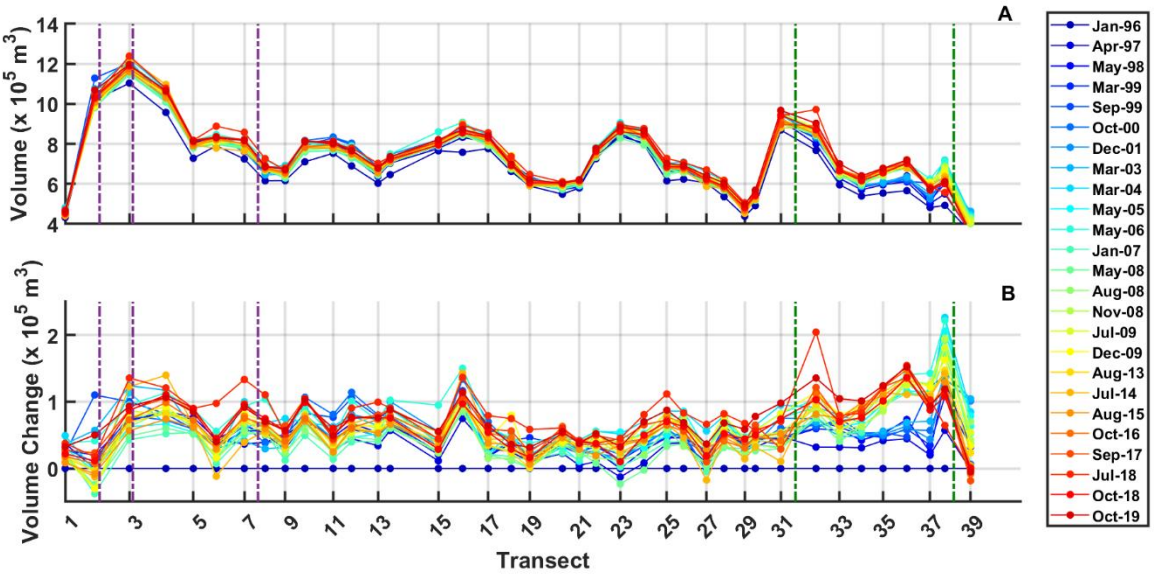

Figure 13: Spatial distribution of total half-cell volume (A) and half-cell volume change (B) of each survey at NMB. Volume change is relative to the initial Jan-96 pre-nourishment survey. Purple vertical lines represent outfall pipes and green vertical lines represent piers. The south side of the study area is associated with Transect 2 while the north side of the study area is associated with Transect 39.

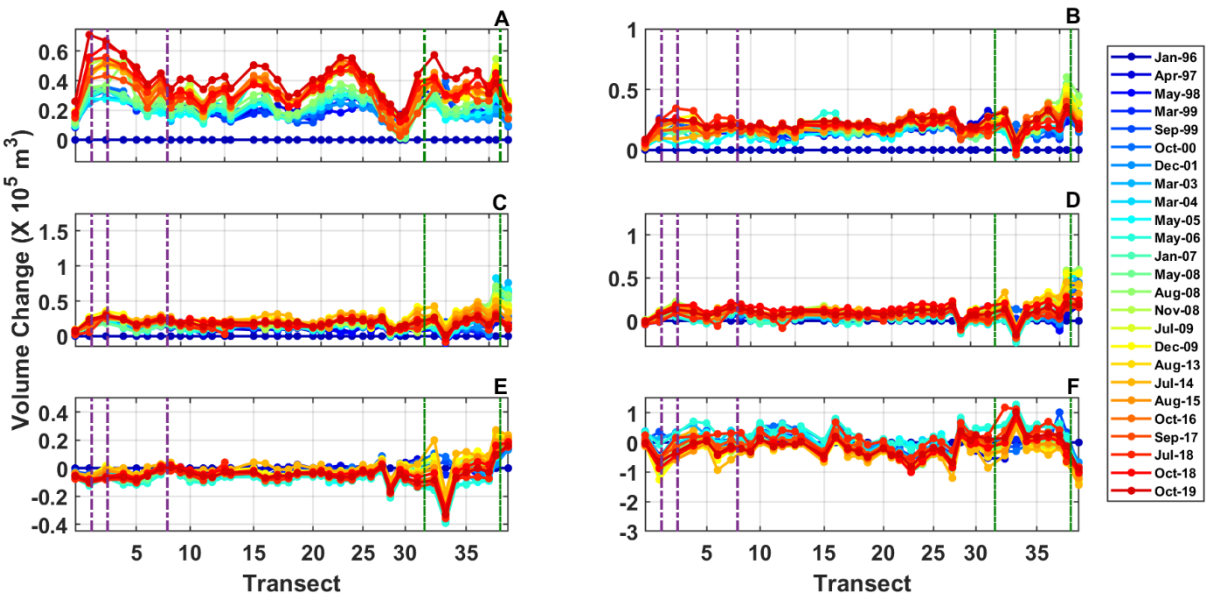

Figure 14: NMB half-cell volume difference by subsection A) Backshore, B) Foreshore, C) Upper Shoreface, D) Lower Shoreface, E) Upper Offshore, and F) Offshore. Volumes differences are referenced to the initial Jan-96 pre-nourishment survey. The south side of the study area is associated with Transect 1 while the north side of the study area is associated with Transect 39. Outfall pipes are distinguished by purple vertical lines while piers are distinguished by green vertical lines.

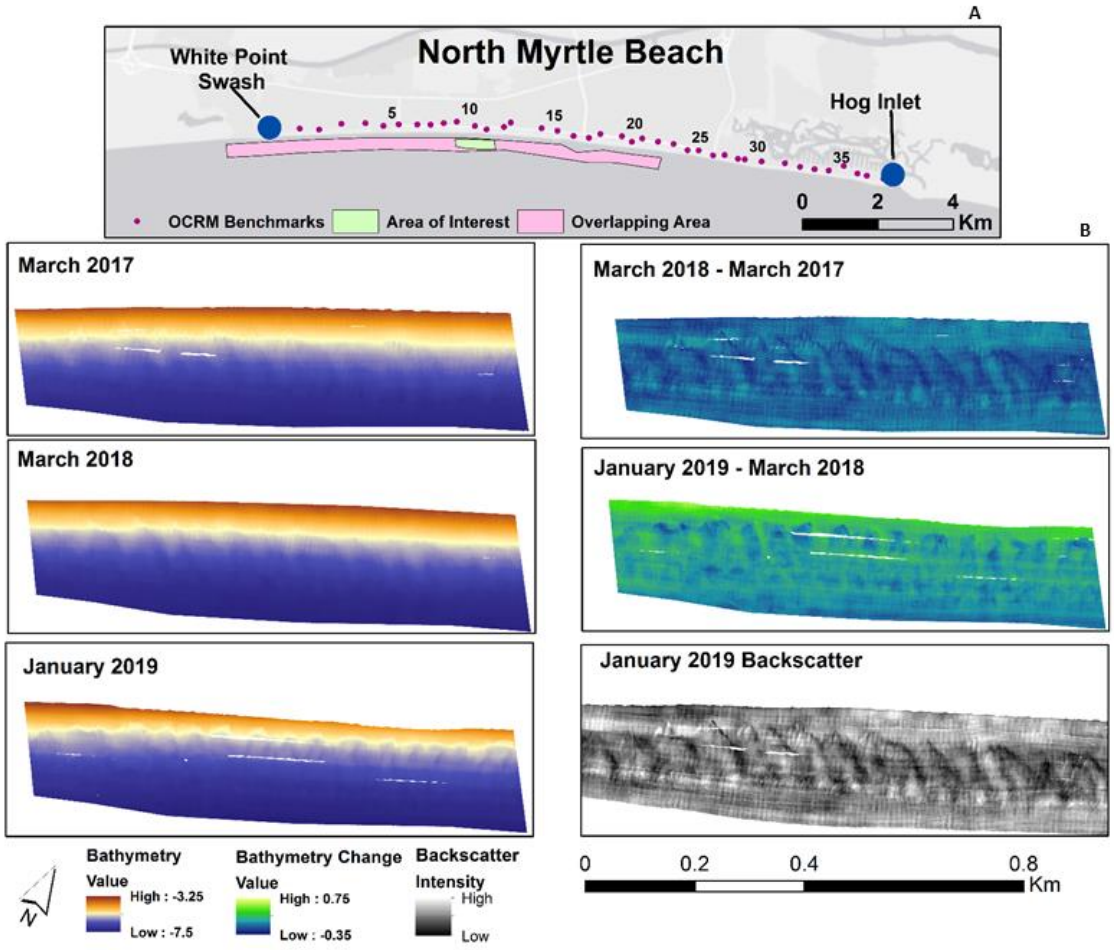

Figure 15: Multibeam bathymetry and backscatter intensity from an area of interest in North Myrtle Beach, SC (surveys March 2017, March 2018, and January 2019) illustrating cuspate features within the lower shoreface-to-shelf transition zone (subset B). Bathymetry differences further highlight these features as volume is typically lost within the features and gained on the limbs of the features. Location of surveys can be found in subset A.

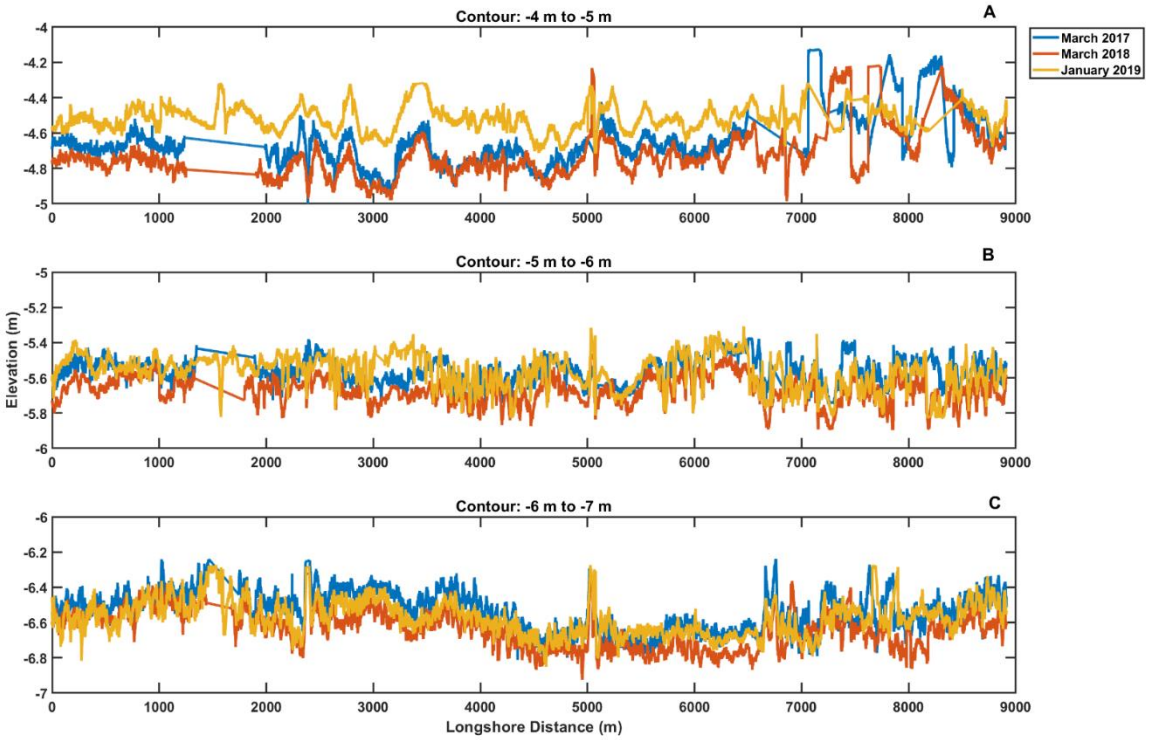

Figure 16: Longshore transects of multibeam bathymetry between contours: -4 to -5m, -5 to -6m, and -6 to -7m which represent the lower shoreface, upper offshore, and offshore subsections.

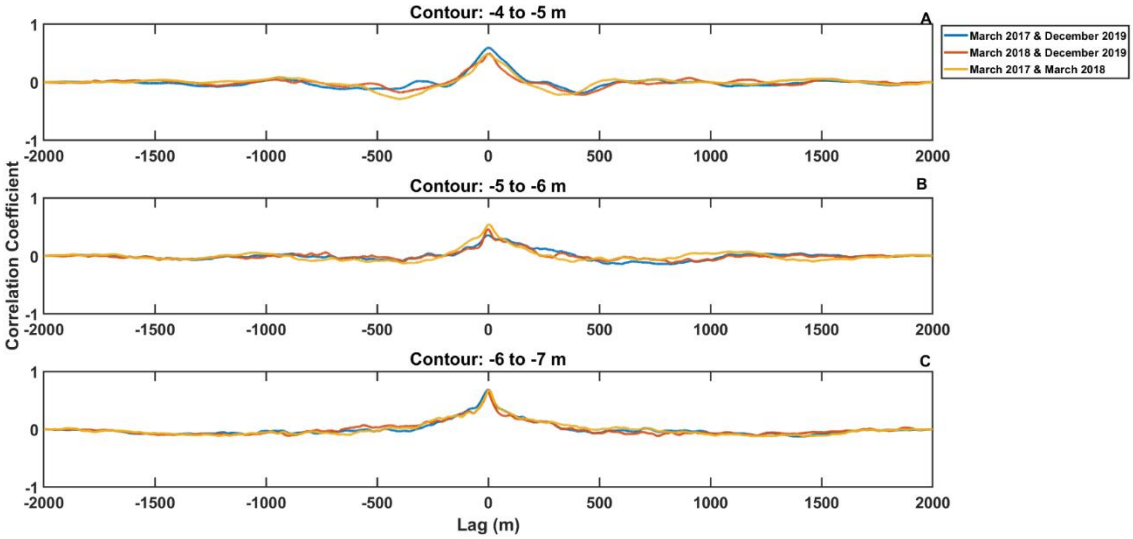

Figure 17: Cross-correlation functions of multibeam bathymetry transects of contour intervals: -4 to -5m, -5 to -6m, and -6 to -7 which represent the lower shoreface, upper offshore, and offshore subsections.

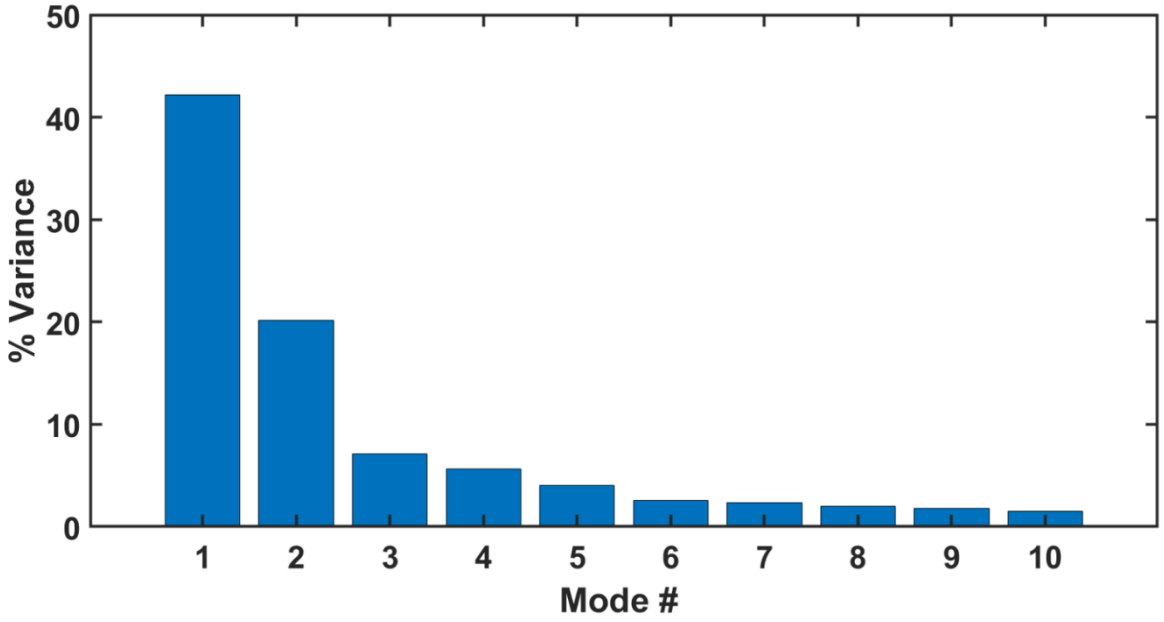

Figure 18: Percent variance of the first ten modes resulting from the EOF analysis of NMB beach mean-removed elevation profiles.

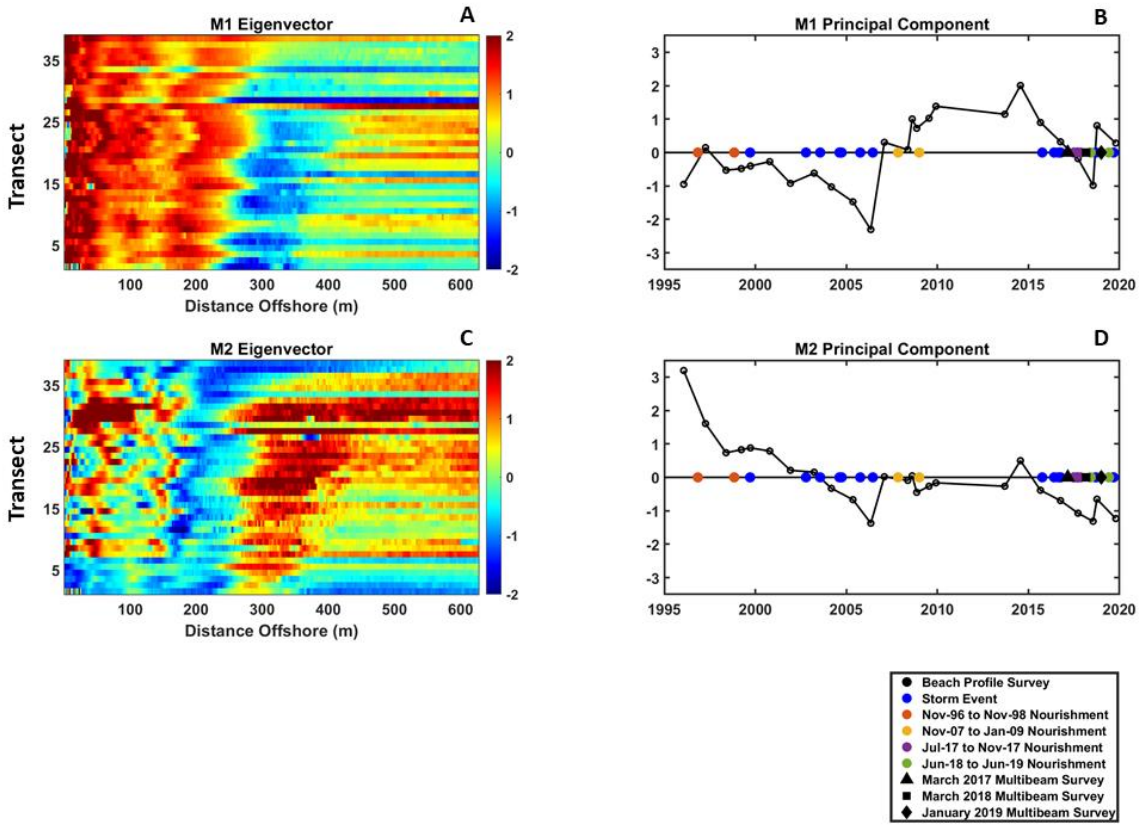

Figure 19: Eigenfunctions and Principal Components for modes one and two resulting from the EOF analysis of the demeaned beach elevation profiles at NMB. Vertical blue lines represent storm events in subset B and D. Timeline of events can be found on the 0 Principal Component value for modes one and two.

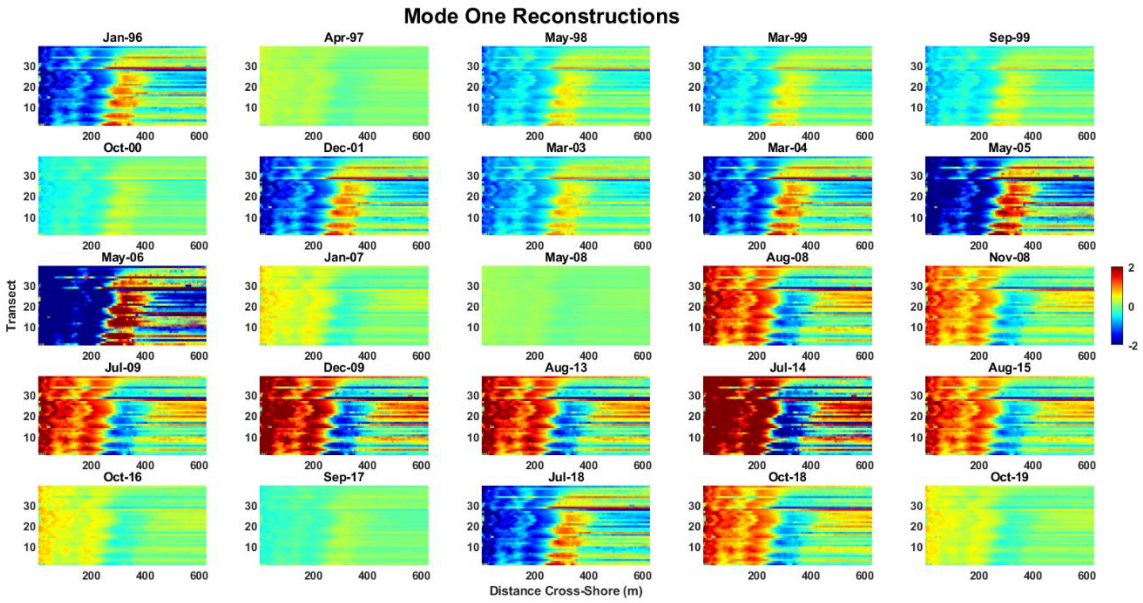

Figure 20: Mode one reconstructions for each survey period.

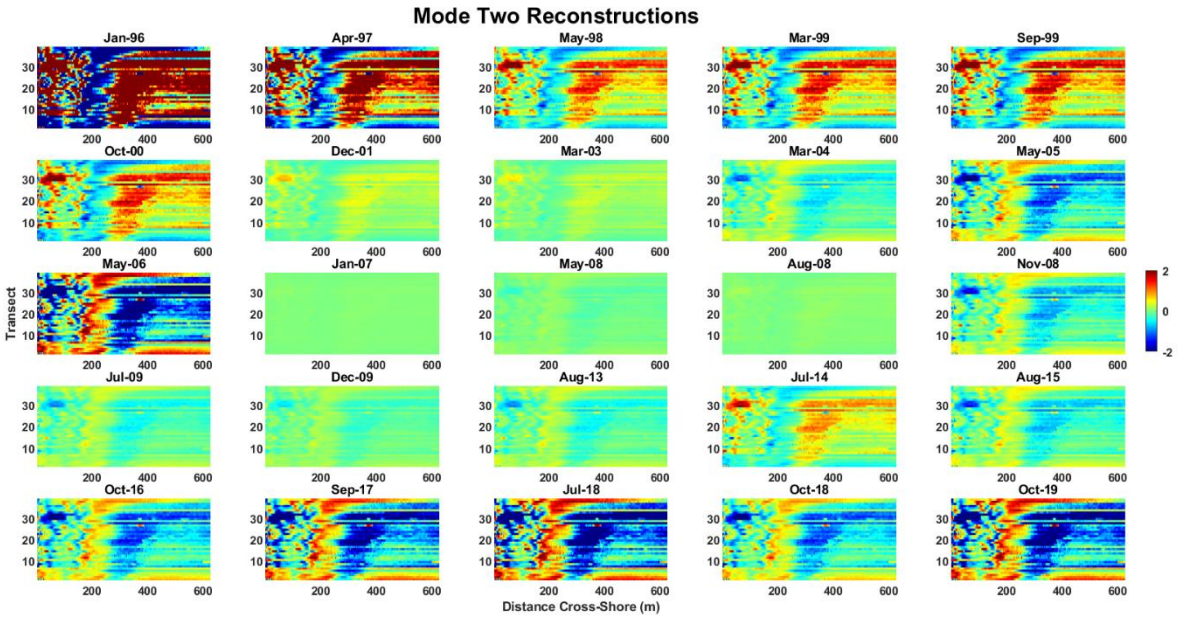

Figure 21: Mode two reconstructions for each survey period.

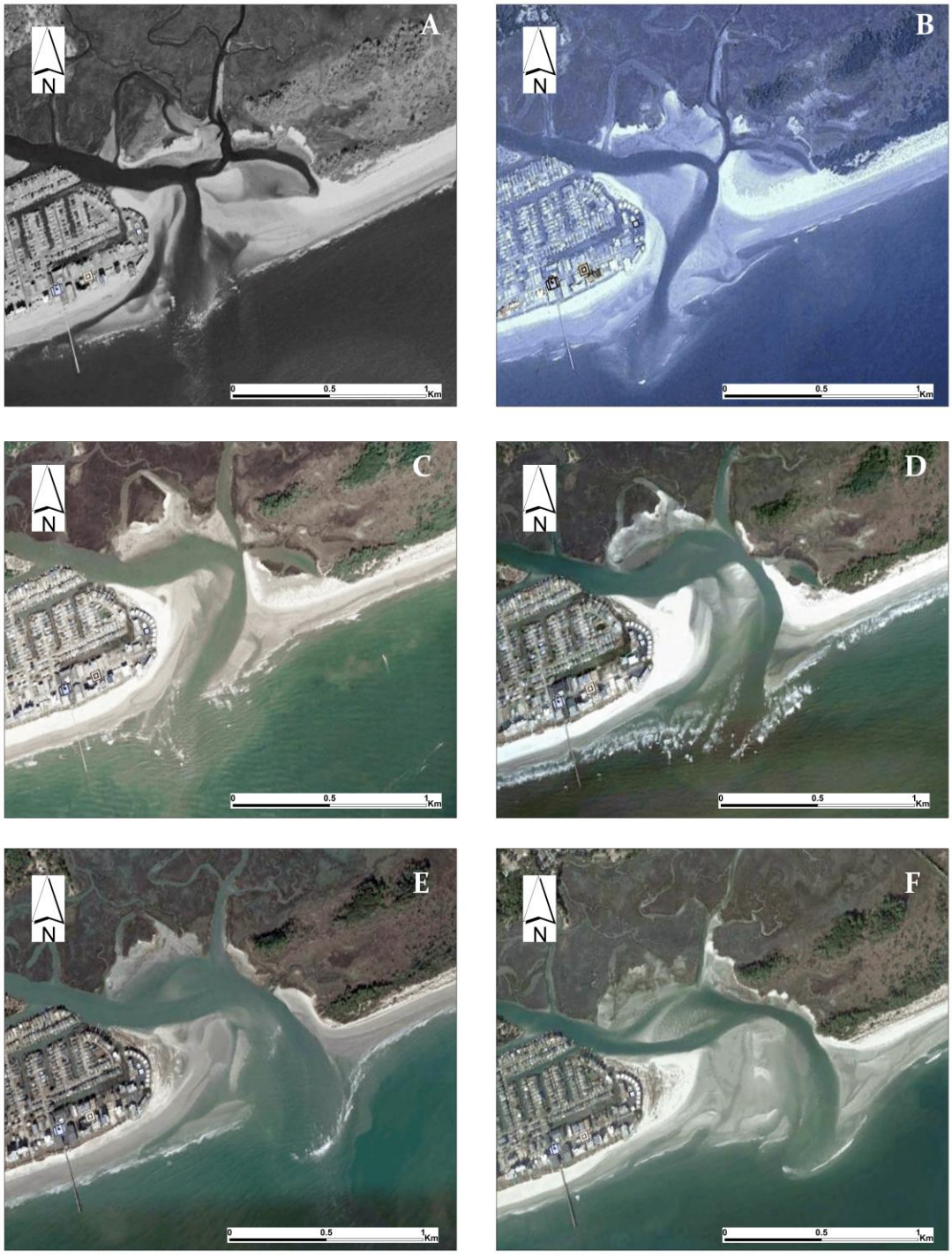

Figure 22: Hog Inlet movement from A) February 1999, B) June 2003, C) October 2007, D) March 2011, E) December 2012, and F) November 2017. Images are referenced in WGS 1984 sourced from Google Earth.

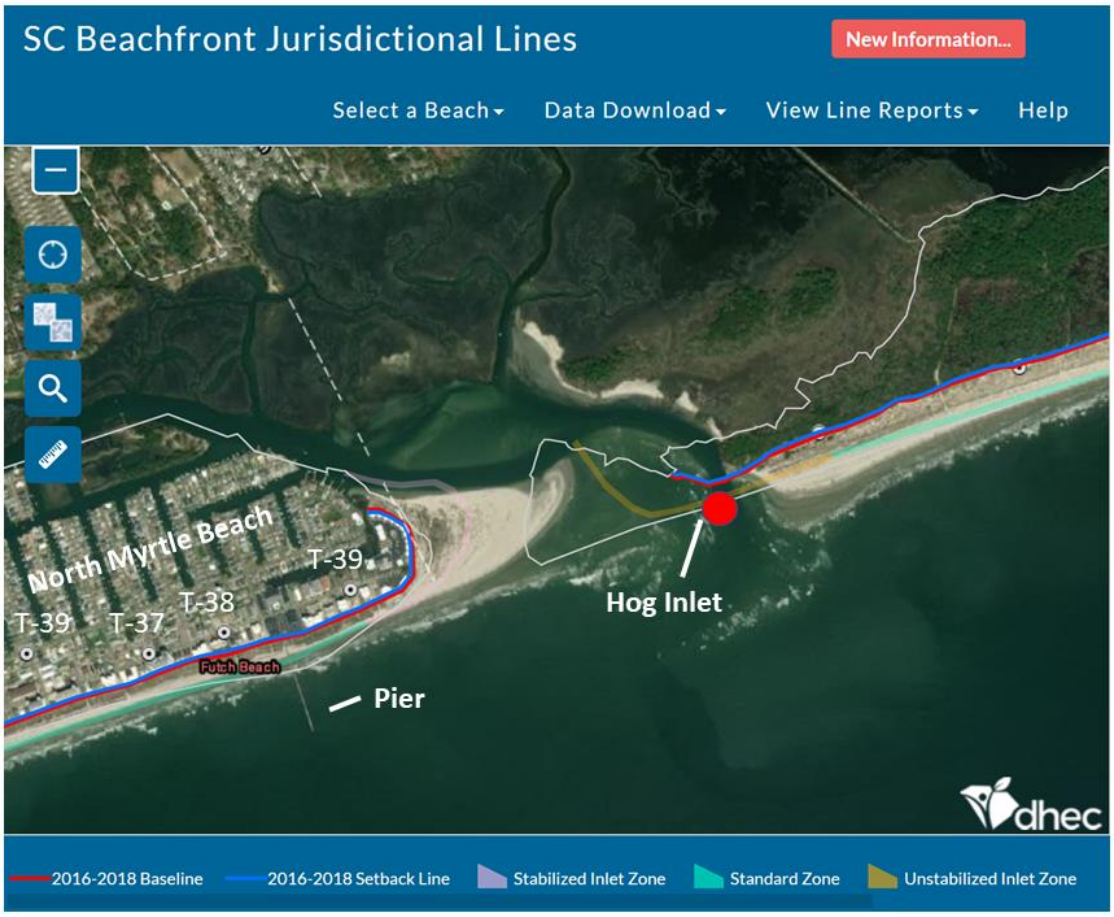

Figure 23: South Carolina Beachfront Jurisdictional Lines. Note that the longshore extent of the stabilized inlet zone for Hog Inlet only reaches T-39. Figure extracted from the SC Department of Health and Environmental Control's website: https://gis.dhec.sc.gov/shoreline/

9. References

1. Aubrey, D. G., and Speer, P. E., (1984) Updrift Migration of Tidal Inlets, *The Journal of Geology*, 92 (5), 531-545

2. Baldwin, J. H., (2008) Variability In Beach Topography and Forcing Along Oak Island, North Carolina (Master's Thesis, University of North Carolina Wilmington, Wilmington, NC).

3. Barnhardt, W., (2009) Coastal Change Along the Shore of Northeastern South Carolina: The South Carolina Coastal Erosion Study. United States Geological Survey, (Circular 1339), 77.

4. Bochev-van der Burgh, L. M., Wijnberg, K. M., and Hulscher, S. J. M. H., (2009) Dune Morphology along a Nourish Coastline, *Journal of Coastal Research*, SI 56 (Proceedings of the 10th International Coastal Symposium), 292 – 296.

5. Cacchione, D. A., Drake, D. D., Grant, W. D., and Tate., G. B., (1984) Rippled scour depression on the inner continental shelf off Central California, *Journal of Sedimentary Petrology*, 54, 1280-1291.

6. Dolan, A. M., (2016) Investigating Coastal Erosion Variability and Framework Geology Influence Along the Grand Strand, South Carolina (Master's thesis, Coastal Carolina University, Conway, SC), Electronic *Theses and Dissertations*. 14.

7. Denny, J.F., Schwab, W.C., Baldwin, W.E., Barnhardt, W.A., Gayes, P.T., Morton, R.A., Warner, J.C., Driscoll, N.W., and Voulgaris, G., (2013) Holocene sediment distribution on the inner continental shelf of northeastern South Carolina: Implications for the regional sediment budget and long-term shoreline response. *Continental Shelf Research*, 56, 56-70.

8. Díez, J., Cohn, N., Kaminsky, G. M., Medina, R., and Ruggiero, P., (2018) Spatial and Temporal Variability of Dissipative Dry Beach Profiles in the Pacific Northwest, U.S.A., *Journal of Coastal Research*, 34, 510 – 523.

9. Dommengent., D. and Latif, M., (2002) A Cautionary Note on the Interpretation of EOFs, Journal of Climate, 15, 2016-225.

10. Farris, A. S., and List, J. H., (2007) Shoreline Change as a Proxy for Subaerial Beach Volume Change, *Journal of Coastal Research*, 23, 740-748.

11. Fredsoe, J. and Deigaard, R. (1992) Mechanics of Coastal Sediment Transport, *River Edge, NJ: World Scientific Publishing*, 396

12. Gayes, P.T., Schwab, W., Driscoll, N.W., Morton, R.A., Baldwin, W.E., Denny, J.J., Wright, E.E., Harris, M.S., Katuna, M.P., Putney, R.T., and Johnstone, E. (2003) Sediment Dispersal Pathways and Conceptual Sediment Budget For A Sediment Starved Embayment: Long Bay, SC, *Coastal sediments '03: "Crossing disciplinary boundaries": the Fifth International Symposium on Coastal Engineering and Science of Coastal Sediment Processes: Proceedings.*

13. Hallermeier, R.J., (1981) A profile zonation for seasonal sand beaches from wave climate. *Coastal Engineering*, 4, 253–277.

14. Hapke C.J., Plant, N.G., Henderson, R.E., Schwab, W.C., and Nelson, T.R., (2016) Decoupling processes and scales of shoreline morphodynamics, *Marine Geology*, 381, 42-53.

15. Hapke, C.J., Kratzmann, M.G., and Himmelstoss, E. A., (2013) Geomorphic and human influence on large-scale coastal change, *Geomorphology*, 199, 160-170.

16. Hapke, C.J., Lentz, E. E., Gayes, P.T., McCoy, C. A., Hehre, R., Schwab, W. C., and Williams, S.J., (2010) A Review of Sediment Budget Imbalances along Fire Island, New York: Can Nearshore Geologic Framework and Patterns of Shoreline Change Explain the Deficit?, *Journal of Coastal Research*, 26, 510 – 522.

17. Kana, T. W., Kaczkowski, H. L., and McKee, P.A., (2011) The 1986–1995 Myrtle Beach nourishment project ten-year performance summary. *Shore & Beach*, 65(1), 8–23.

18. Kana, T.W., Traynum, S. B., Gaudiano, D., Kaczkowski, H. L., and Hair, T., (2013) The Physical Condition of South Carolina Beach 1980-2010, *Journal of Coastal Research*, SI, 69, 61-82.

19. Kraus, N.C., and Harikai, S., (1999), Numerical model of the shoreline change at Oarai Beach, *Coastal Engineering*, 7-1, 1-28.

20. Kulp, S. and Strauss, B., (2019) New elevation data triple estimates of global vulnerability to sea-level rise and coastal flooding, Natural Communications, 10(1), 1-12

21. Larson, M., and Kraus, N. C., (1994) Temporal and spatial scales of beach profile change, Duck, North Carolina. *Marine Geology*, 117, 75-94.

22. Lemke, L., Miller, J.K., Gorton, A., and Livermont, E., (2014) EOF Analysis Of Shoreline Changes Following an Alternative Beachfill Within a Groin Field, Coastal Engineering, 1- 12

23. Ludka, B. C., Guza, R. T., O'Reilly, W. C., and Yates, M. L., (2015) Field evidence of beach profile evolution towards equilibrium, *Journal of Geophysical Research: Oceans*, 120, 7574 – 7597.

24. McCoy, C., Hill, J., Gayes, P., Marshall, J., Okano, S., Johnson, B., Howe, M., and Klotsko, S., (2010) 2007 – 2010 Grand Strand Beach Nourishment Study: Final Report, US Army Corps of Engineers, Charleston District

25. Miller, J.K., and Dean, R.G., (2007) Shoreline variability via empirical orthogonal function analysis: Part 1 temporal and spatial characteristics, Coastal Engineering, 54, 111-131.

26. Morang A., Birkemeier W.A. (2005) Depth of Closure on Sandy Coasts. In: Schwartz M.L. (eds) Encyclopedia of Coastal Science. Encyclopedia of Earth Science Series. Springer, Dordrecht. https://doi.org/10.1007/1-4020-3880-1_116

27. Murray, A. B., and E. R. Thieler (2004), A new hypothesis and exploratory model for the formation of large-scale inner-shelf sediment sorting and ‘‘rippled scour depressions,’’ *Cont. Shelf Res*., 24, 295 – 315

28. Neumann, B., Vafeidis, A., Zimmermann, J., and Nicholls, R.J., (2015), Future Coastal Population Growth and Exposure to Sea-Level Rise and Coastal Flooding – A Global Assessment

29. Park, J.-Y., Gayes, P.T., and Wells, J.T., (2009) Monitoring Beach Nourishment along the Sediment-Starved Shoreline of Grand Strand, South Carolina, *Journal of Coastal Research*, 25, 336-349.

30. Short, A. D., Bracs, M. A., and Turner, I. L., (2014) Beach oscillation and rotation: local and regional response at three beaches in southeast Australia, *Journal of Coastal Research*, Special Issue 70, 712-717

31. Slovinsky, P., (2001) Spatial Variation of Beach Morphology Along Coastal South Carolina. Columbia, South Carolina: Department of Geology, University of South Carolina, Master's thesis, 166pp.

32. South Carolina Code of Laws, Title 48-Environmental Protection and Conservation, Chapter 39, Coastal Tidelands and Wetlands, Section 48-39-270 access: https://www.scstatehouse.gov/code/t48c039.php

33. South Carolina Floodwater Commission, State of South Carolina (2019) *South Carolina Floodwater Commission Report November 8, 2019*. https://governor.sc.gov/sites/default/files/Documents/Floodwater%20Commission/SCFWC%20Report.pdf

34. Southgate, H. N., Wijnberg, K. M., Larson, M., Capobianco, M., and Jansen, H., (2003) Analysis of Field Data of Coastal Morphological Evolution over Yearly and Decadal Timescales. Part 2: Non-Linear Techniques, *Journal of Coastal Research*, 19, 776-789.

35. Theuerkauf, E. J., and Rodriguez, A. B., (2012) Impacts of Transect Location and Variations Along-Beach Morphology on Measuring Volume Change, *Journal of Coastal Research*, 28, 707-718.

36. Warner, J. C., Armstrong, B., Sylvester, C. S., Voulgaris, G., Nelson, T., Schwab, W. C., and Denny, J. F., (2012), Storm-induced inner-continental shelf circulation and sediment transport: Long Bay, South Carolina, *Continental Shelf Research*, 42, 51-63

37. Weisberg, R.H. and Pietrafesa, L.J. (1983) Kinematics and Correlations of Surface Winds in the South Atlantic Bight. Journal of Geophysical Research, Oceans, 88, C8 4593–4610

38. Weisberg, R.H. and Pietrafesa, L.J. (1982). Revelations of the Kinematical Motions and Cross-Correlations of South Atlantic Bight Surface Winds from three Coastal Wind Stations and three Offshore Oceanic Marine Buoys. North Carolina State University - Center for Marine & Coastal Studies Technical Report No. 83-1-1, 89 numbered pages.

39. Willson, K., Thomson, G., Roberts Briggs, T., Elko, N., and Miller, J., (2017) Beach nourishment profile equilibration: What to expect after sand is placed on a beach, ASBPA White Paper, *Shore & Beach*, 85-2, 49-51